**Kopriva, David Alan**

# A STREAM FUNCTION METHOD FOR COMPUTING STEADY ROTATIONAL TRANSONIC FLOWS WITH APPLICATION TO SOLAR WIND-TYPE PROBLEMS

*The University of Arizona* PH.D. 1982

# A STREAM FUNCTION METHOD FOR COMPUTING STEADY ROTATIONAL TRANSONIC FLOWS WITH APPLICATION TO SOLAR WIND-TYPE PROBLEMS

by

David Alan Kopriva

---

A Dissertation Submitted to the Faculty of the

PROGRAM IN APPLIED MATHEMATICS

In Partial Fulfillment of the Requirements
For the Degree of

DOCTOR OF PHILOSOPHY

In the Graduate College

THE UNIVERSITY OF ARIZONA

1 9 8 2

THE UNIVERSITY OF ARIZONA
GRADUATE COLLEGE

As members of the Final Examination Committee, we certify that we have read the dissertation prepared by David Alan Kopriva

entitled A Stream Function Method for Computing Steady Rotational Transonic Flows with Application to Solar Wind-Type Problems

and recommend that it be accepted as fulfilling the dissertation requirement for the Degree of Doctor of Philosophy.

| | |
|---|---|
| | May 6, 1982 Date |
| | " " Date |
| | " " Date |
| | " " Date |
| | Date |

Final approval and acceptance of this dissertation is contingent upon the candidate's submission of the final copy of the dissertation to the Graduate College.

I hereby certify that I have read this dissertation prepared under my direction and recommend that it be accepted as fulfilling the dissertation requirement.

| | |
|---|---|
| Dissertation Director | 5/6/82 Date |

STATEMENT BY AUTHOR

This dissertation has been submitted in partial fulfillment of requirements for an advanced degree at the University of Arizona and is deposited in the University Library to be made available to borrowers under rules of the Library.

Brief quotations from this dissertation are allowable without special permission, provided that accurate acknowledgement of source is made. Requests for permission for extended quotation from or reproduction of this manuscript in whole or in part may be granted by the head of the major department or the Dean of the Graduate college when in his judgement the proposed use of the material is in the interests of scholarship. In all other instances, however, permission must be obtained from the author.

Signed: 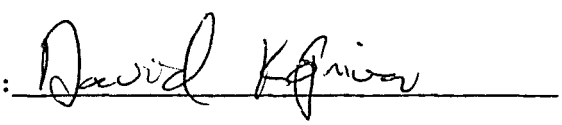

## ACKNOWLEDGMENTS

Like any other dissertation, this work was not performed in a total vacuum. Over the past few years many people have helped out both directly and indirectly.

It was Randy Jokipii's suggestion of computing galactic winds that led to my study of transonic flows and formed the starting focus of this dissertation. In addition, he supplied me with all the creature comforts a student could need - especially the latest in computer gadgetry and plenty of computer funds. Most of all, under Randy I was able to pursue my own ideas no matter where they led.

The suggestion of using a stream function to look at the wind problem came from Dick Seebass. I don't think he expected me to take his suggestion as far as I did, but it didn't take long to see that it would provide a unique view of the problem.

It is always nice to have people around off whom I could bounce the many dumb ideas I am constantly coming up with. Joe Davila took the brunt of these for a full year. Then he moved out of the office and never came back. Since then, "Sri" Sritharan has performed that valuable role. This is the only thanks they get for an otherwise thankless job.

I must also thank Dr. Seebass and the other members of the committee for the NASA Computational Fluid Dynamics Traineeship. The fellowship provided me with opportunities I otherwise would not have. As part of the deal, the CFD branch at NASA Ames had to put up with me

for a summer and I thank Harv Lomax and his group for their hospitality and encouragement.

A requirement of the Applied Math Department is that each dissertation be reviewed by an outside reader. I would like to thank Dr. E. N. Parker for taking the time from his busy schedule to comment on my work.

Finally, I say thanks to all my friends who most often did their best to keep me from working. Some like Pete, Dave, Diane, and Mark have already left. Others, like Ron, Peter, John, Karen, Joe and Vikki continue their task (with varying success) which should be a lot easier now that this is done.

TABLE OF CONTENTS

LIST OF ILLUSTRATIONS

LIST OF ILLUSTRATIONS -- continued

## LIST OF SYMBOLS

| | |
|---|---|
| $a$ | sound speed |
| $P$ | pressure |
| $q$ | gas speed $(u^2+v^2+w^2)^{1/2}$ |
| $u,v,w$ | physical velocity components |
| $V_i, V^i$ | covariant and contravariant velocity components |
| $M$ | Mach number |
| $h_i$ | geometric scale factor |
| $g_{ij}$ | metric tensor |
| $c$ | azimuthal velocity function |
| $C$ | correction |
| $J$ | Jacobian |
| $f$ | mass flux |
| $L$ | differential operator |
| $G$ | universal gravitational const. |
| $Q$ | speed in azimuthal plane $(u^2 + v^2)^{1/2}$ |
| $s_c$ | critical radius |
| $g$ | gravitational force |
| $S$ | entropy |
| $A,B$ | geometric coefficients in stream function equation |
| $R_s, R_n$ | coefficients for supersonic relaxation scheme |
| $T$ | temperature, artificial time, azimuthal trans. fn. |
| $t$ | artificial time |
| $E$ | parameter for eccentricity of oblate spheroid |
| | |
| $\rho$ | density |
| $\psi$ | stream function |
| $\phi$ | gravitational potential |
| $\gamma$ | polytropic index |
| $\omega$ | relaxation parameter |
| $\zeta$ | vorticity |
| $M$ | source mass |
| $L$ | characteristic length |
| $\xi$ | shock position or characteristic |
| $\Omega$ | open region or angular frequency |
| $\theta$ | latitude |
| $\phi$ | azimuthal angle |

Coordinate systems:

| | |
|---|---|
| $(x,y,z)$ | Cartesian |
| $(X,Y,\phi)$ | Computational |
| $(s,n)$ | streamwise-normal |
| $(y^1,y^2,y^3)$ | curvilinear |

ABSTRACT

A numerical scheme has been developed to solve the quasilinear form of the transonic stream function equation. The method is applied to compute steady two-dimensional axisymmetric solar wind-type problems. A single, perfect, non-dissipative, homentropic and polytropic gas-dynamics is assumed. The four equations governing mass and momentum conservation are reduced to a single nonlinear second order partial differential equation for the stream function. Bernoulli's equation is used to obtain a nonlinear algebraic relation for the density in terms of stream function derivatives. The vorticity includes the effects of azimuthal rotation and Bernoulli's function and is determined from quantities specified on boundaries.

The approach is efficient. The number of equations and independent variables has been reduced and a rapid relaxation technique developed for the transonic full potential equation is used. Second order accurate central differences are used in elliptic regions. In hyperbolic regions a dissipation term motivated by the rotated differencing scheme of Jameson is added for stability. A successive-line-overrelaxation technique also introduced by Jameson is used to solve the equations.

The nonlinear equation for the density is a double valued function of the stream function derivatives. The velocities are extrapolated from upwind points to determine the proper branch and

Newton's method is used to iteratively compute the density. This allows accurate solutions with few grid points.

The applications first illustrate solutions to solar wind models. The equations predict that the effects of vorticity must be confined near the surface and far away the streamlines must resemble the spherically symmetric solution. Irrotational and rotational flows show this behavior. The streamlines bend toward the rotation axis for rapidly rotating models because the coriolis force is much larger than the centrifugal force.

Models of galactic winds are computed by considering the flow exterior to a surface which surrounds a uniform density oblate spheroid. Irrotational results with uniform outward mass flux show streamlines bent toward the equator and nearly spherical sonic surfaces. Rotating models for which Bernoulli's function is not constant show the sonic surface is deformed consistant with the one-dimensional theory.

# CHAPTER 1

## INTRODUCTION

We have developed a numerical scheme to solve the quasilinear form of the transonic stream function equation and apply the method to rapidly compute steady two-dimensional solar wind-type problems. In flows with spherical symmetry, the theory of the solar wind describes the expansion against the pull of gravity of an essentially static atmosphere to supersonic speeds. We show the more general two-dimensional axisymmetric problem can be characterized by a vorticity introduced by rotation and variations of Bernoulli's function and entropy. The stream function approach to these problems is a new and general way to extend the quasi one-dimensional theory developed by Parker(1958,1963). In recent years there has been interest in computing wind type flows from galaxies which are two-dimensional in nature (Bregman, 1978; Habe and Ikeuchi, 1980; Bardeen and Berger, 1978) and we apply the method to these types of problems too.

Because the use of the stream function reduces the four equations of mass and momentum conservation to a single second order partial differential equation, there is also a computational incentive to develop stream function algorithms. At the time we began, however, no technique was available to solve the transonic stream function equation. The availability of such a technique is important for it would enable the rapid and direct solution of rotational steady

transonic flows. Therefore we present a method for solving the stream function equation in quasilinear form. Because this has not been done in detail in the past, our discussion will be not be limited specifically to the application of the wind problem.

The stream function formulation and its numerical solution will be discussed in the first part of this work. After the technique described here was developed, Hafez and Lovell(1981) presented a successful stream function technique for solving external flows over bodies. Our approach differs from theirs. They solved their problem in a form which explicitly conserved vorticity while we solve the quasilinear form. Also, the method they developed for computing the density from the stream function cannot be used for internal flows or the wind-type applications. Our method is simple, reliable, and can be used for such problems.

For the second part we will solve a stream function formulation of some "wind" models. Numerical solutions of rotational and irrotational solutions for both "stellar" and "galactic" models will be presented to show the utility of using the stream function approach for the theoretical study of such problems.

The use of the stream function represents a middle ground between two commonly used methods for solving steady transonic flows. First, time marching techniques for the Euler equations or Reynolds-averaged Navier-Stokes equations have been used effectively to solve a wide variety of transonic flows for many years. But time marching techniques are currently inefficient for computing steady flows (Lomax,1981). For many flows of interest, however, the potential

approximation is accurate and efficient relaxation techniques for solving the transonic potential equation have been developed in the past ten years. (See, for example, Ballhaus, Jameson and Albert, 1978; Schmilovich and Caughey, 1981.) Nevertheless, the presence of vorticity produced by shocks or introduced by "swirling" (Batchelor, 1967) motions in axisymmetric flows invalidates the potential approximation. The attraction of the stream function approach is that the rapid relaxation techniques developed for the transonic potential equation could be used without the restrictive assumption of irrotationality.

The stream function has not been used for transonic computations, however, for two reasons. First, the stream function equation is of mixed type. That is, it is elliptic in subsonic flows, hyperbolic in supersonic flows, and parabolic at the sonic line. Systematic iterative methods to solve mixed-type equations were not fully developed until the early 1970's. Second, and in recent years most important, systematic methods for computing the density from the stream function derivatives were not recognized.

Through work on the potential equation, the solution of mixed type equations is now routine. The breakthrough for solving such equations came from Murman and Cole(1971) who introduced type-dependent differencing schemes for the solution of the transonic small disturbance potential equation. In subsonic flows, standard central differences were used. In supersonic regions, however, the streamwise derivatives were upstream differenced. The shifting of derivatives

effectively added a dissipative term which stabilized the scheme. Jameson(1974) developed a method based on this idea that could be used for the full potential equation. He also analysed relaxation methods that could be used to solve the difference equations. We have applied these ideas to solve the stream function equation.

The reason why the velocity potential and not the stream function has been used in the past is because of the density problem. In the potential formulation, the density is defined uniquely by the gradient of the potential. The gradient of the stream function, however, represents the mass flux and not the velocity. As a function of the mass flux the density is double valued. One value corresponds to supersonic flow, the other to subsonic. It is only now through this work and that of Hafez and Lovell(1981) that systematic methods for computing the density have been recognized.

So it is not surprising that there have been few attempts to solve the transonic stream function equation. In three papers, Emmons(1944,1946,1948) did solve flows in ducts and over airfoils with a relaxation technique based on the recent work of Southwell(1940). Emmons' hand relaxation approach allowed him to circumvent the two major obstacles described above. But twenty years later, Allen and Sadler tried to develop a computer code based on Emmons' method and the supercritical flow results were unsatisfactory (Hall, 1981).

A small disturbance stream function method for subcritical and supercritical flows over airfoils was published by Chin and Rizzetta(1979). The equation was formulated so that there was no ambiguity in the type of the equation and the density problem was

circumvented. The type dependent differencing scheme of Murman and Cole(1971) was used. Still, a method for solving the stream function equation for arbitrary flows did not exist.

Finally, Hafez and Lovell(1981) have presented a general technique for solving the vorticity equation form of the stream function equation. They computed flows about a cylinder and a 10% parabolic arc airfoil. Their results finally show that the use of the stream function can be a viable technique.

The applications with which we demonstrate our scheme are quite different. They are characterized by the smooth acceleration of a uniformly subsonic flow to a uniformly supersonic one. Flows in two-dimensional nozzles or ducts with no back pressure are representative examples. One-dimensional models for the ablation of hydrogen pellets in plasmas show an acceleration from subsonic to supersonic flow due to a combination of geometric expansion and external heat addition(e.g. Parks and Turnbull, 1978). Similarly, in the solar wind, the effects of gravity and the geometrical expansion of the streamlines combine to create an effective nozzle through which the gas is accelerated to supersonic speeds.

The mathematical theory of the spherically symmetric solar wind assuming a polytropic gas was developed by Parker(1958) well before satellite measurements confirmed its existence. Since then, the model has been refined with the addition of the effects of magnetic fields, viscosity, and heat conduction. Reviews of the

theory and observations are numerous so we only point out the books by Parker(1963) and Hundhausen(1972).

In its simplest one-dimensional form, the solar wind theory reduces to an examination of Bernoulli's equation and the conservation of mass. This is a convenient form in which to examine the problem, for the value of Bernoulli's constant determines the existence and position of a sonic transition. As Parker(1963) has shown, the same ideas extend to more than one dimension.

The problem with the quasi one-dimensional results of Parker comes from the fact that the streamlines are not in general known. Consequently, two or three-dimensional problems have been examined in a number of ways. Pneuman and Kopp(1971), for instance, assumed a magnetic field distribution and assumed the streamlines followed the field lines. The flow properties along each streamline were computed. From them, the current was found. Finally, Ampere's law derived a new field configuration. This procedure was iterated until the field no longer changed. Perturbation methods have also been used. Siscoe and Finley(1969), for instance, linearized the equations about the spherically symmetric solutions to obtain latitude variations of the solar wind. Finally, time dependent relaxation processes represent the most general approach. While most place their boundaries in the supersonic regions as Pizzo(1978,1980,1981) does, some, such as Endler(1971) have computed transonic flows.

The same basic theory would apply to the expansion of gas from a galaxy. The major difference between galactic models and the

stellar ones is that for the former the sources of mass are distributed in volume. One dimensional models of "galactic winds" can be found in Burke(1968), Johnson and Axford(1971), Holzer and Axford(1970) and Ipavich(1975). Time dependent calculations have been made by Mathews and Baker(1971).

The theory of two-dimensional axisymmetric flow from non-spherical objects such as disks is not well developed. Bardeen and Berger(1978) assumed self-similarity and computed flows from disk galaxies. They placed an inflow boundary beyond the source region so the problem was much like a solar wind flow. Admittedly, the self-similarity assumption was quite restrictive but they were able to find transonic solutions. Unlike the spherically symmetric flow, the transonic flow varied continuously with changes in the velocity with which the gas was emitted. Unfortunately, solutions did not exist within a cone about the symmetry axis.

Two studies which use time dependent methods have been published. The first was that of Bregman(1979) who used a "Fluid in Cell" (FLIC) method developed by Black and Bodenheimer(1975) to solve the flow from a distributed gas source representing a galaxy. Models which had an inflow boundary beyond the source region were solved for galactic winds by Habe and Ikeuchi(1980) using a first order method called the "beam scheme" (Van Albada, Van Leer, and Roberts, 1981; Sanders and Prendegrast, 1974).

By using the stream function formulation we take a new and different approach which is used for both the solar and galactic wind problems. It is important because it also allows for the extension of

the ideas of the one-dimensional theory to two dimensional axisymmetric flows. In particular, the one dimensional theory accounts only for variations in the magnitude of the total enthalpy. Through the stream function formulation, this and the effects of two dimensional variations can be studied. The effects of rotation and vorticity also appear explicitly. We feel that this important information is missed in the earlier studies by using the primitive variables.

Our stream function formulation also has the advantage of solving the steady problem directly. First, solutions can be found much more rapidly than with a time dependent approach. On a more fundamental level, the boundary conditions are more clear and are motivated by the theory of second order partial differential equations. For time dependent techniques, the proper specification of boundary conditions requires considerable care. (See, for instance, Oliger and Sunstrom, 1978.) For two-dimensional flows, three quantities are required to be specified at the inflow and none at the outflow for the "wind" problem. The results of Habe and Ikeuchi(1980) are particularly suspect because, according to their paper, only the two conditions of temperature and density were specified along the inflow boundary.

Finally, our approach to the applications will be exploratory in nature. We solve two-dimensional irrotational and rotational solar wind flows which both show the performance of the numerical technique and which present examples of the two-dimensional characteristics

which can be inferred from the stream function equation. For galactic models we present examples of flows from uniform density oblate spheroidal bodies. The parameters which are used are chosen for convenience and not for any particular physical reason. Consequently, no inferences will be made regarding observational implications.

Outline

The plan of this work is to present in Chapter 2 the basic gas-dynamics equations and from them derive the stream function equations for the steady transonic flow problems. Other aspects of the formulation such as the vorticity, the double valued density function, and the mathematical properties of the equations are also discussed in Chapter 2. In Chapter 3 the numerical technique used to solve the equations is developed.

Up to this point the presentation is fairly general. The applications are then examined in Chapter 4. The first section introduces the one-dimensional theory of wind-type problems. In the second, the solar wind problem is extended to two-dimensional axisymmetric flows. Solutions to such problems are shown in the third section. The final section covers briefly an extension to non-radial gravitational forces and non-spherical sources - galactic wind models - for which no one-dimensional theory exists.

# CHAPTER 2

## THE STREAM FUNCTION FORMULATION

In this chapter we formulate the steady rotational transonic flow problem in terms of a stream function. Because transonic computations with the stream function have not yet been discussed in detail, the approach will be fairly general. For the most part, the results will be independent of the specific applications to be considered in Chapter 4 or of computational considerations discussed in Chapter 3. The goal is to present a self-contained derivation and analysis of the gas-dynamics and stream function equations to form a basis for the numerical solution of particular flow problems.

We begin in section 2.1 by presenting the gas physics and equations which will be assumed throughout this work. The discussion is limited to axisymmetric flows in section 2.2 where we define the stream function and derive the equations it must satisfy. In section 2.3 the vorticity is derived in a form consistent with the stream function formulation. The difficulty with using the stream function, however, comes from the computation of the density. In section 2.4 we discuss the nature of the density function computed in terms of the stream function. The mathematical properties of the stream function equations are discussed in section 2.5. Particular attention will be paid to those properties which will influence the development of

numerical methods. Finally, in section 2.6 we discuss the boundary conditions to be used for the stream function.

## 2.1 Gas Dynamics Equations

The basic gas dynamics equations which will be used throughout the following chapters are collected here. For the stream function formulation is is most convenient to use concepts of vorticity and Bernoulli's equation than to be limited to the conservation form of the Euler equations. The flows that we consider occur in an open region $\Omega \subset \mathbf{R}^3$ exterior to a closed surface $S$. Completely enclosed by $S$ will be a source of gas and gravity. (See figure 2.1.) All gas in $\Omega$ will result from flow out of $S$ which will be called the "base".

We first make a number of commonly used simplifications to the gas physics. First, we assume a flow composed of a single, perfect, and non-dissipative gas. For the convenience of not having to specify an extra set of parameters for the entropy, the flow is assumed to be homentropic. The assumption that the gas is polytropic with index $\gamma$ will crudely take into account effects of heating and thermal conduction. Self gravitation of the gas should be negligible and will be ignored. We do, however, allow for the sources and hence the gas, to rotate about some axis through $S$.

Under the assumptions above, the steady gas flow in $\Omega$ is described by the Euler equations

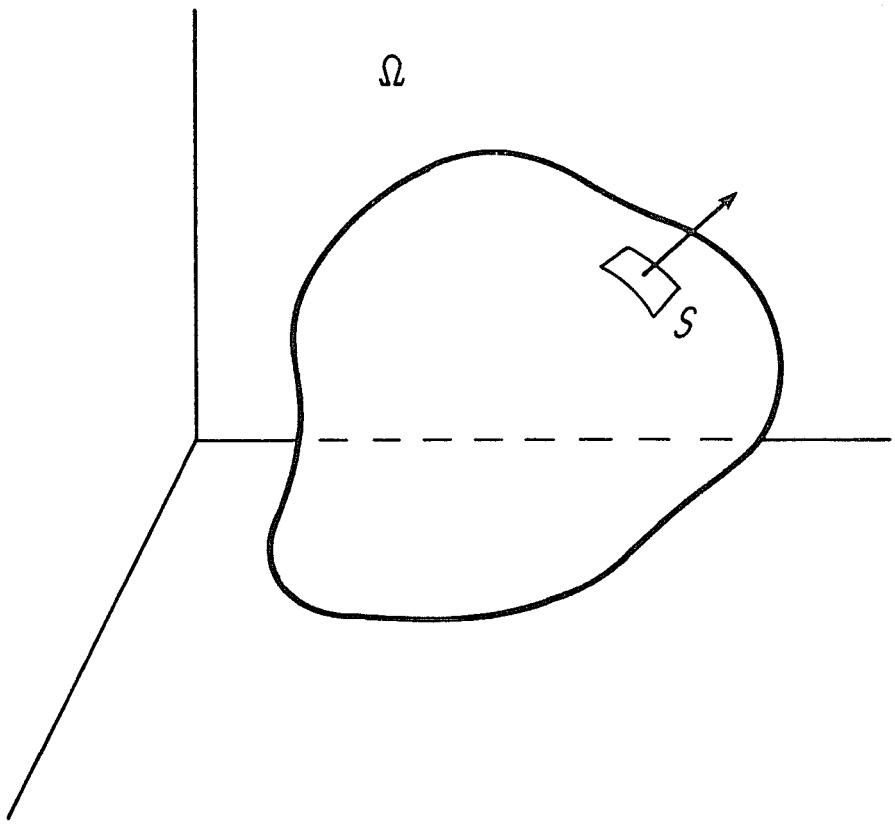


Fig. 2.1 The basic flow geometry --- Gas flows out of the three dimensional surface $S$ which completely surrounds a source of gas and gravity.

$$\overline{\nabla}\cdot\overline{\rho \underline{q}} = 0 \tag{2.1}$$

$$\overline{\nabla}\cdot\overline{\rho \underline{q}\underline{q}} + \overline{\nabla P} + \overline{\rho \nabla \Phi} = 0 \tag{2.2}$$

$$\overline{P} \propto \overline{\rho}^{\gamma} \tag{2.3}$$

Where $\overline{\rho}$ is the density, $\overline{\underline{q}}$ is the velocity, $\overline{P}$ is the pressure and $\overline{\Phi}$ is the gravitational potential. The overbar notation indicates a dimensional quantity.

Before proceeding further, equations (2.1) - (2.3) will be scaled. Let $\Phi_o = GM/L$ where $M$ is the source mass, $L$ is a characteristic length. Let $\rho_o$ be a characteristic density. With these, define

$$\rho = \overline{\rho}/\rho_o \qquad \Phi = \overline{\Phi}/\Phi_o$$

$$\underline{q} = \overline{\underline{q}}/(\Phi_o)^{1/2} \qquad \nabla = L\overline{\nabla}$$

Then equations (2.1)-(2.3) will appear just as they do above but without the overbars.

Since the flow is non-dissipative and steady (but not necessarily irrotational) Bernoulli's equation can be used to rewrite the conservation form above to a form which will be more useful later. Using the vorticity

$$\underline{\zeta} = \nabla \times \underline{q} \tag{2.4}$$

equation (2.2) can be written in non-conservation form as

$$\frac{1}{2}\nabla q^2 - \underline{q} \times \underline{\zeta} + \frac{a^2}{\rho}\nabla\rho + \nabla\Phi = 0 \tag{2.5}$$

where $a^2 = ( \partial P/\partial \rho )_S = \gamma P/\rho = a_0^2 \rho^{\gamma-1}$ is the square of the scaled sound speed. Integrating (2.5) along a streamline gives Bernoulli's equation

$$\frac{1}{2} q^2 + \frac{a^2}{\gamma-1} + \phi = H \tag{2.6}$$

where H, which may vary between streamlines, is the Bernoulli function. For the special case where $\gamma = 1$, i.e. the flow is isothermal, Bernoulli's equation becomes

$$\frac{1}{2} q^2 + a^2 \log\rho + \phi = H \tag{2.7}$$

Rearranging (2.5), it can be seen that

$$\underline{q} \times \underline{\zeta} = \nabla H \tag{2.8}$$

which is Crocco's theorem in homentropic flow (Batchelor, 1967 p. 160). If the flow was not assumed to be homentropic, the right hand side of eqn. (2.8) would be modified by subtracting $T\nabla S$ where T is the temperature. Thus, eq. (2.1) - (2.3) can be rewritten as

$$\nabla \cdot \rho \underline{q} = 0 \tag{2.9a}$$

$$\frac{1}{2} \nabla q^2 + a^2 \frac{\nabla \rho}{\rho} + \nabla( \Phi - H) = 0 \tag{2.9b}$$

$$\frac{1}{2} q^2 + \frac{a^2}{\gamma-1} + \phi = H \tag{2.9c}$$

## 2.2 The Stream Function

The basic idea behind using a stream function is to define a function such that the continuity equation (2.9a) is identically satisfied. In 2-dimensional or axisymmetric geometries this can be done with a single scalar function $\psi$ . Consistent with the applications we wish to consider later, we will assume $S$ and all flow parameters are cylindrically symmetric about some axis which will correspond to the rotation axis for rotating problems.

To allow for the computation of flows in complex geometries, we will first make our definitions in a general curvilinear coordinate system. Let the vector $x^i=(x^1,x^2,x^3)$ be a fixed cartesian coordinate. To take advantage of axisymmetry choose a curvilinear coordinate system given by $y^i=(y^1,y^2,y^3)$ so that the $y^2=0$ axis corresponds to the symmetry axis. The $y^3$ axis is chosen as the azimuthal angle about $y^2$ so there are no variations in the $y^3$ direction. This effectively reduces the problem to two dimensions in $(y^1,y^2)$.

Using the Einstein summation rule, define the metric of the transformation between $x^i$ and $y^i$ by

$$g_{ij} = \frac{\partial x^\alpha}{\partial y^i}\frac{\partial x^\alpha}{\partial y^j} \tag{2.10}$$

and the Jacobian by $g = \det(g_{ij}) = J^2$. Without loss of generality, we can require orthogonality between the $y^3$ and the other axes so that $g_{3j}=0$, $j \neq 3$. Call the contravariant velocity vector $V^i$. Then equation (2.9a) becomes

$$(\rho JV^1)_{y1} + (\rho JV^2)_{y2} = 0 \tag{2.11}$$

Let $\psi(y^i)$ be the stream function defined through the relations

$$\begin{aligned} \psi_{y1} &= -\rho JV^2 \\ \psi_{y2} &= \rho JV^1 \end{aligned} \tag{2.12}$$

Then, interpreting the derivatives in the sense of distributions, $\psi$ identically satisfies eq. (2.11).

The momentum equations (2.9b) are next reduced to a single second order partial differential equation for $\psi$. One approach is to form a combination of the $y^1$ and $y^2$ components of the equations (2.5). This is straightforward for viscous flows and other cases, say, where magnetic fields are present. For polytropic gases an easier formulation is through the vorticity equation (2.4). The $y^3$ component of the vorticity is

$$-\frac{1}{J}((V_1)_{y2} - (V_2)_{y1}) = \zeta_3 \tag{2.13}$$

where $V_i = g_{ij}v^j$ are the covariant velocity components. Substituting for $V_1$ and $V_2$,

$$(g_{11}V^1 + g_{12}V^2)_{y2} - (g_{21}V^1 + g_{22}V^2)_{y1} = -J\,\zeta_3 \tag{2.14}$$

Substituting the definitions eqns. (2.12) into eqn (2.14) gives the stream function equation

$$\left(\frac{g_{11}\psi_{y2} - g_{12}\psi_{y2}}{\rho J}\right)_{y2} - \left(\frac{g_{21}\psi_{y2} - g_{22}\psi_{y1}}{\rho J}\right)_{y1} = -J\zeta_3 \qquad (2.15)$$

Since the problems in Chapter 4 will involve flows where spherical and oblate spheroidal coordinates are natural, we will actually compute later in an orthogonal coordinate system $y^i=(X,Y,\phi)$ where the metric tensor reduces to the diagonal $g_{ij}=h_{ii}^2= h_i^2$. For example, a stretched spherical coordinate system could be given by the transformation

$$\begin{aligned} x &= F(X)\cos(T(Y))\sin(\phi) \\ y &= F(X)\cos(T(Y))\cos(\phi) \\ z &= F(X)\sin(T(Y)) \end{aligned} \qquad (2.16)$$

where F(X) and T(Y) are the radial and latitudinal stretching functions, respectively.

In orthogonal coordinates the continuity equation can be written in terms of the physical velocity components (u,v,w) as

$$(\rho h_2 h_3 u)_X + (\rho h_1 h_3 v)_Y = 0 \qquad (2.17)$$

Leading to the definitions

$$\begin{aligned} \psi_X &= -\rho h_1 h_3 v \\ \psi_Y &= \rho h_2 h_3 u \end{aligned} \qquad (2.18)$$

And the vorticity equation becomes

$$\frac{\partial}{\partial X}\left(\frac{h_2\psi_X}{\rho h_1 h_3}\right) + \frac{\partial}{\partial Y}\left(\frac{h_1\psi_Y}{\rho h_2 h_3}\right) = -h_1 h_2 \zeta_3 \qquad (2.19)$$

In the following discussions, we will refer only to the orthogonal case.

For reasons discussed in section 3.1 the quasilinear form of eq. (2.19) which does not explicitly contain density derivatives is used in the computations. By definition, quasilinear means that the equation is linear in the highest derivatives of $\psi$ and the coefficients of those derivatives are functions of position and lower order derivatives only. Equation (2.19) can be written in quasilinear form by expanding the derivatives and substituting for the density derivatives using Bernoulli's equation. If we define $A = (h_1 h_3)^{-1}$ and $B = (h_2 h_3)^{-1}$ the expanded vorticity equation is

$$(Ah_2\psi_X)_X + (Bh_1\psi_Y)_Y - Ah_2\psi_X(\log\rho)_X - Bh_1\psi_Y(\log\rho)_Y = -\rho h_1 h_2 \zeta_3 \qquad (2.20)$$

The logarithmic density derivatives are obtained by differentiating Bernoulli's equation. Let $Q^2 = u^2 + v^2$ be the square of the velocity component in the (X,Y) plane. Then

$$d(\log\rho) = \frac{1}{a^2-Q^2}\left(H'd\psi - \frac{1}{2\rho^2}(d(A\psi_X)^2 + d(B\psi_Y)^2) - d\Phi - \frac{1}{2}dw^2\right) \qquad (2.21)$$

where the prime denotes differentiation with respect to the argument. Substituting for $(\log\rho)_X$ and $(\log\rho)_Y$, rearranging and multiplying by the factor $\rho(a^2 - Q^2)h_3$ yields the quasilinear form

$$\frac{(a^2 - u^2)\psi_{XX}}{h_1^2} - \frac{2uv\psi_{XY}}{h_1 h_2} + \frac{(a^2 - v^2)\psi_{YY}}{h_2^2}$$
$$- \frac{\rho v h_3}{h_1}\left[\left(\frac{h_1}{h_1}\right)_X(u^2 - a^2) + \left(\frac{h_2}{h_2}\right)_X(a^2 - 2u^2 - v^2) - \left(\frac{h_3}{h_3}\right)_X a^2\right]$$
$$+ \frac{\rho u h_3}{h_2}\left[\left(\frac{h_1}{h_1}\right)_Y(a^2 - u^2 - 2v^2) + \left(\frac{h_2}{h_2}\right)_Y(v^2 - a^2) - \left(\frac{h_3}{h_3}\right)_Y a^2\right] \qquad (2.22)$$
$$- \frac{\rho v h_3}{h_1}\left[\Phi_X + \frac{1}{2}(w^2)_X - H'\psi_X\right] + \frac{\rho u h_3}{h_2}\left[\Phi_Y + \frac{1}{2}(w^2)_Y - H'\psi_Y\right]$$
$$= \rho(Q^2 - a^2)h_3\zeta_3$$

From the derivation, then, we see that this quasi-linear form is obtained from the vorticity equation multiplied by $\rho(a^2 - Q^2)h_3$.

## 2.3 Vorticity

The four equations represented by eqn. (2.9a) and (2.9b) have now been reduced to a single second order partial differential equation for $\psi$. In the process, a new quantity - the vorticity - has been introduced. How $\zeta_3$ and the azimuthal velocity w are computed is discussed in this section. The advantage of the stream function formulation and of solving the steady problem in particular is that $\zeta_3$ and w are determined by $H(\psi)$ and a new quantity $c(\psi)$ which are specified on boundaries only. Batchelor(1967, p. 543), for example, computes these for incompressible flow.

First, because of the axisymmetry, we can derive a relation for w along each streamline. The third component of Crocco's equation, eq. (2.8) is

$$u\zeta_2 - v\zeta_1 = 0 \tag{2.23}$$

From the definition of the vorticity

$$\begin{aligned} \zeta_1 &= \frac{1}{h_1 h_3}(h_3 w)_X \\ \zeta_2 &= -\frac{1}{h_2 h_3}(h_3 w)_Y \end{aligned} \tag{2.24}$$

Substitute these into eq. (2.23) to obtain

$$\underline{q}\cdot\nabla(h_3 w) = 0 \tag{2.25}$$

so that

$$w = \frac{c(\psi)}{h_3} \tag{2.26}$$

where c is a function constant along streamlines. To get the vorticity, the first component of Crocco's equation (2.8) is

$$v\zeta_3 - w\zeta_2 = \frac{1}{h_1} H'(\psi)\psi_X \tag{2.27}$$

Substitute for $\zeta_2$, w and v using (2.24), (2.26), and (2.18) to obtain

$$\zeta_3 = -\rho(H' h_3 - cc'/h_3) \tag{2.28}$$

## 2.4 The Density Function

The major source of difficulty in using the stream function formulation is the computation of the density which must be obtained from Bernoulli's equation. Sells(1968) studied the problem much as we do here. In terms of the stream function the density can be expressed through

$$\rho^{\gamma-1} = \frac{\gamma-1}{a_o^2}\left(H - \Phi - \frac{1}{2}(c/h_3)^2\right) - \frac{\gamma-1}{2\rho^2}\left((\psi_X/h_1h_3)^2 + (\psi_Y/h_1h_3)^2\right) \quad (2.29)$$

To examine the properties of this equation let

$$H^* = \frac{\gamma-1}{a_o^2}\left(H - \Phi - \frac{1}{2}(c/h_3)^2\right) \quad (2.30)$$

$$f^2 = \frac{\gamma-1}{a_o^2}\left((\psi_X/h_1h_3)^2 + (\psi_Y/h_2h_3)^2\right) \quad (2.31)$$

The function f is proportional to the mass flux. Then

$$\rho = \left(H^* - \frac{f^2}{2\rho^2}\right)^{1/\gamma-1} \quad (2.32)$$

The most important result is that for f less than some critical value the density is double valued. Figure 2.2 shows an example of the density versus f for four values of $\gamma$ with $H^*$ chosen so that the maximum value of $\rho = 1$.

The maximum flux point - the turning point when the density becomes single-valued - corresponds to $a^2 = Q^2$. In terms of the equation

$$0 = \rho^{\gamma-1} + \frac{f^2}{2\rho^2} - H^* \quad (2.33)$$

the minimum $(\partial\rho/\partial f)^{-1} = 0$ corresponds to the turning point. The derivative is

$$\rho_f = -fa_o^2/(\rho(\gamma-1)(a^2-Q^2)) \quad (2.34)$$

Not only does the turning point occur at $a^2 = Q^2$, the upper branch corresponds to elliptic flows and the lower to hyperbolic flows.

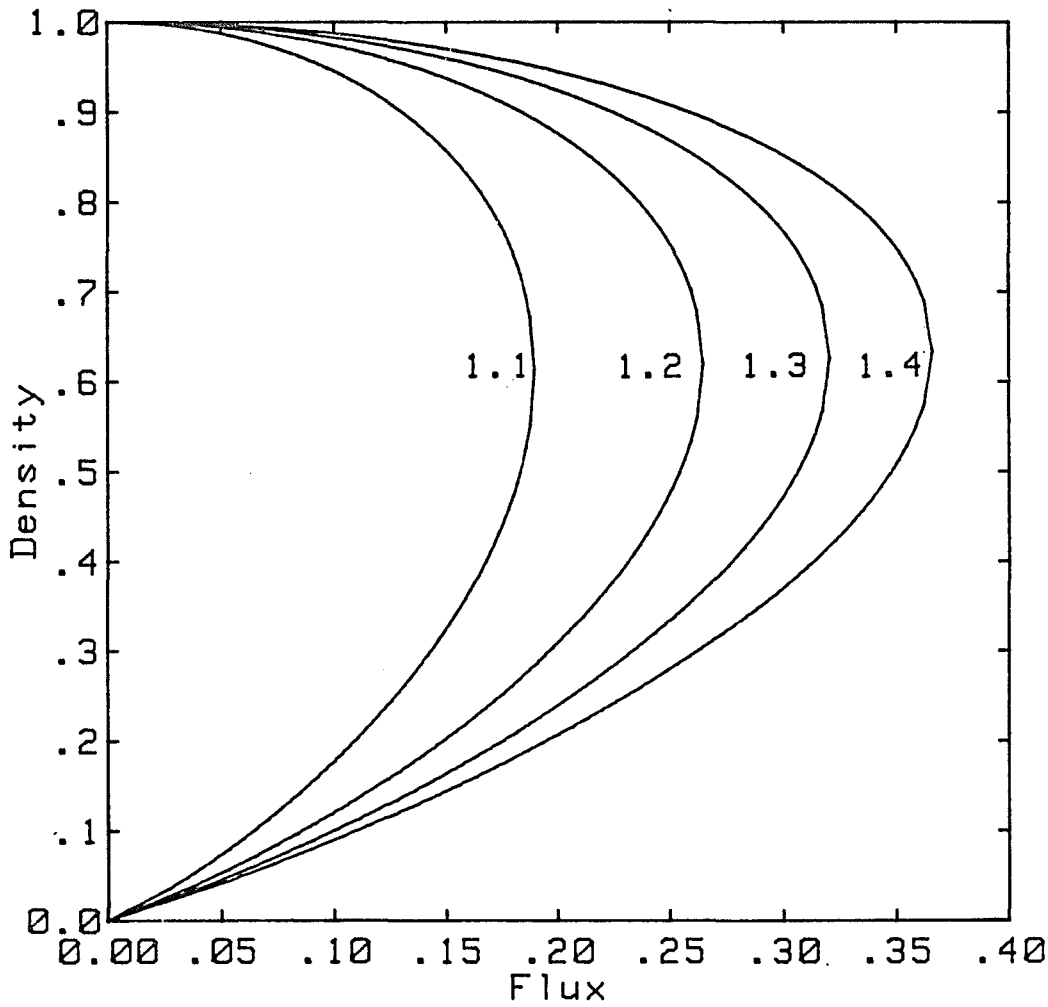


Fig. 2.2 The density as a function of mass flux for four values of $\gamma$

The choice of branch at a particular point in space must be made by considering other conditions. In particular, the fact that expansion shocks violate the entropy condition (see Lax,1973, for example) means a jump from the upper to the lower branch cannot be allowed. Also, shocks must satisfy the Rankine-Hugoniot relations. For practical considerations, the necessity of choosing between two branches of the non-linear algebraic equation (2.32) can be avoided by realizing that the density is a single-valued function of the speed $Q^2$

$$\rho = ( H^* - (\gamma-1)\, Q^2/a_o^2)^{1/\gamma-1} \qquad (2.35)$$

and the difficulty is shifted to finding $Q^2$ , conditions on which are imposed by the Rankine-Hugoniot relations at shocks and by continuity elsewhere.

## 2.5 Mathematical Properties

The two most important properties of equations (2.19) and (2.22) that should be discussed are their mixed type and their weak solutions. Both look much like their counterparts for the conservative and quasilinear potential equations. The potential equation, however, expresses the mass conservation equation and the potential identically satisfies the vorticity equation. The stream function equation expresses the vorticity equation and identically satisfies the continuity equation. Even so, in smooth flow the equations for the potential and the stream function have similar properties. The fact that the required shock conditions are different, though, will indicate that facts associated with the

solution of the potential equations do not necessarily relate to the stream function equations.

Type of the Stream Function Equation

Both equations (2.19) and (2.22) are of mixed type depending upon the magnitude of the velocity in an azimuthal plane. According to the theory of second order partial differential equations in two variables (see Courant and Hilbert, 1962) the type of a differential operator of the form

$$Lu = au_{xx} + 2bu_{xy} + cu_{yy} \qquad (x,y)\in\mathcal{D} \subset \mathbf{R}^2 \qquad (2.36)$$

where $u\in C^2(\mathcal{D})$ and $a,b,c\in C^0(\mathcal{D})$ is determined by the number of real characteristics. The slopes of these characteristics are given by

$$\xi_{\pm} = \left.\frac{dy}{dx}\right|_{\pm} = \frac{-b \pm (b^2 - ac)^{1/2}}{a} \qquad (2.37)$$

Equation (2.36) is hyperbolic if there are two real characteristics, parabolic if there is one, and elliptic if there are none. It is within this framework that we analyse eq. (2.19) and (2.22).

For simplicity, choose cylindrical coordinates in which to work. The highest order terms of eq. (2.22) are

$$L_q = (\psi_X{}^2 - (\rho aY)^2)\psi_{YY} - 2\psi_Y\psi_X\psi_{XY} + (\psi_Y{}^2 - (\rho aY)^2)\psi_{XX} \qquad (2.38)$$

so the characteristic slopes are

$$\xi_{\pm} = \frac{-uv \pm (Q^2 - a^2)^{1/2}}{u^2 - a^2} \qquad (2.39)$$

The type of the operator does not necessarily change when the flow is subsonic or supersonic. Rather, it is dependent upon the magnitude of the projected speed $Q^2 = u^2 + v^2$.

The characteristics for the vorticity equation are identical to those of the quasilinear form. The highest order terms are

$$L_v = L_q/(\gamma^3\rho^3(Q^2 - a^2)) \tag{2.40}$$

so the characteristic slopes $\xi_{\pm}$ are just those in equation (2.39).

Finally, we note that the characteristics of the stream function equations represented in eq. (2.39) are the same as those of the potential equation because the coefficients are the same. The importance of this is that the numerical schemes for solving the potential equation in hyperbolic regions can also be used for the stream function equations.

Weak Solutions

If one extends the class of allowable solutions to discontinuous flows, care must be taken to choose only the proper weak solutions. For gas dynamic flows these are solutions whose discontinuities satisfy the Rankine-Hugoniot relations. (See, for example, Courant and Friedrichs, 1948.) For illustration we will now work in two-dimensional cartesian coordinates to show what weak solutions are satisfied by the stream function.

The important gas dynamic discontinuities are shocks. Let $\xi(x,y)$ denote the shock slope $(dy/dx)_{shock}$. Then integrating eqns. (2.1) and (2.2) gives the shock jump conditions (Hafez and Lovell, 1981)

$$\begin{aligned} [\rho u]\xi + [\rho v] &= 0 \\ [\rho u^2 + P]\xi + [\rho uv] &= 0 \\ [\rho v^2 + P]\xi + [\rho uv] &= 0 \end{aligned} \tag{2.41}$$

where $[\cdot]$ denotes the jump in a quantity across a shock. The stream function was chosen to satisfy the continuity equation identically so the first relation is automatically satisfied. The second two can be expressed in terms of $q_t$ and $q_n$, the velocity components normal and tangential to a shock, as

$$[\rho q_n^2 + P] = 0 \tag{2.42}$$

$$[q_t] = 0 \tag{2.43}$$

The normal momentum condition is satisfied by introducing a jump in the entropy across the shock. The second condition is implied by the vorticity equation (2.13). Integrating the general equation over a volume $\mathcal{D}$ across which runs a shock,

$$\int_{\mathcal{D}} \frac{\partial V_1}{\partial y^2} - \frac{\partial V_2}{\partial y^1}\, dy^1 dy^2 = \int_{\mathcal{D}} -J\zeta_3 dy^1 dy^2 \tag{2.44}$$

If $H'(\psi)$, which is specified by boundary conditions, is continuous, equation (2.28) for $\zeta_3$ shows the integrand is characterized by a jump

discontinuity along the shock. Thus, the associated jump condition is simply

$$[V_1]\xi - [V_2] = 0 \tag{2.45}$$

which expresses (2.43).

Equation (2.19) by itself expresses this requirement since it is nothing more than a re-expression of the vorticity. Notice, however, that the quasilinear equation can admit non-physical solutions. As an example, the two-dimensional cartesian form of the quasilinear equation is

$$(a^2 - u^2)\psi_{xx} - 2uv\psi_{xy} + (a^2 - v^2)\psi_{yy} = 0 \tag{2.46}$$

if the flow is irrotational. A solution of (2.46) on $\mathbf{R}^2$ is

$$\begin{aligned} \psi(x,y) &= bx \\ \rho(x,y) &= \begin{cases} \rho_{sub} & x < x_o \\ \rho_{sup} & x > x_o \end{cases} \end{aligned} \tag{2.47}$$

where b and $x_o$ are constants. The densities $\rho_{sub}$ and $\rho_{sup}$ are chosen from the subsonic and supersonic branches of the density function, respectively. This solution corresponds to a uniform flow in the y-direction with a "shock" which lies along a streamline. Since the pressure (through the density) is not continuous across the $x_o$ streamline the solution does not represent a contact discontinuity. Furthermore, such a solution is rotational and does not satisfy eq. (2.19).

Just because the quasilinear form of the equation admits what appear to be non-allowed jumps does not mean that the form is not useful. The conservation law relates jumps in the velocities, not the stream function derivatives. One possibility to avoid solutions such as (2.47) is to compute u and v and hence $\rho$ from the vorticity equation in such a way that (2.45) is satisfied. This problem is considered in more detail in section 3.1.

## 2.6 Boundary Conditions

The problems solved in Chapter 4 will require three types of physical boundary conditions. At the base, inflow conditions are specified. Since the computational mesh extends only a finite distance from the base, some outflow condition will be needed. The third type of condition must be supplied along symmetry boundaries. Mathematically, the choice of boundary conditions must be made consistent with the second order mixed-type nature of the stream function equation. In the absence of rigorous theoretical results for this particular problem, we propose the use of the following boundary conditions.

Suppose that the base $S$ has both the rotational symmetry about the Y axis and a plane of symmetry perpendicular to that axis. Thus, only a quarter plane problem need be solved as shown in figure 2.3. By choice of the coordinate system (X,Y) the boundary curves $C_1$ and $C_2$ lie along lines of constant X. The symmetry boundaries $S_1$ and $S_2$ lie on constant Y lines. The outer curve $C_2$ is considered only because the computational mesh is finite.

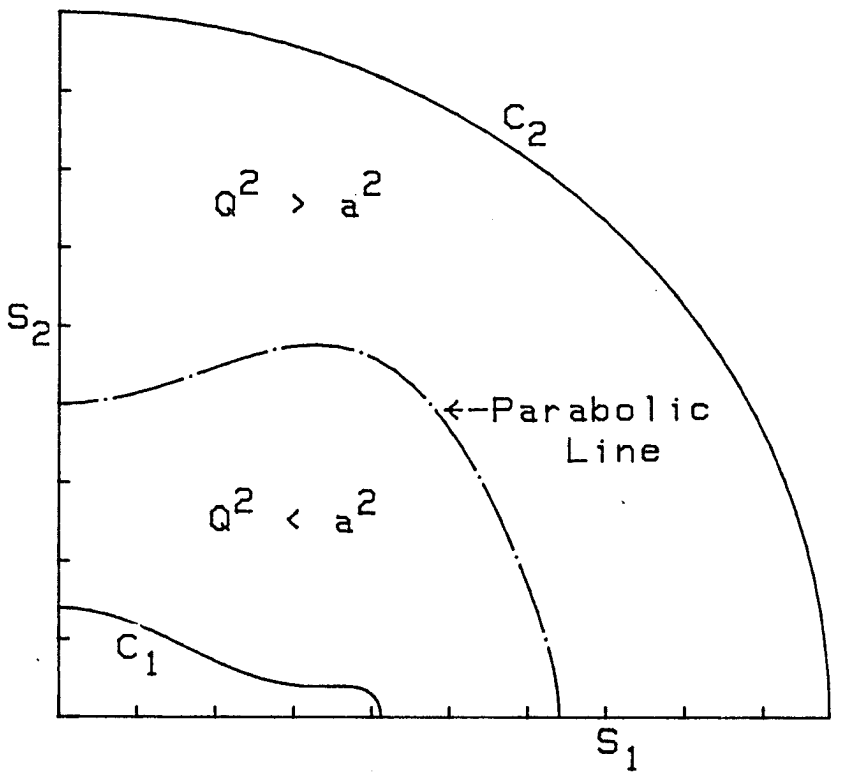


Fig. 2.3 The two-dimensional quarter-plane problem --- $C_1$ is the inflow boundary corresponding to the projection of $S$ onto the (X,Y) plane. $C_2$ is the artificial outflow boundary. $S_1$ and $S_2$ are symmetry boundaries. $S_1$ is the rotation axis for rotating flows.

The symmetry axes $S_1$ and $S_2$ must be streamlines. Thus, the boundary conditions $\psi$ = constant are specified there. For convenience, $\psi = 0$ along $S_1$. The flow near the base, $C_1$, is subsonic. Specifying either the normal derivative $\psi_n$ or the function $\psi$ is presumed to be acceptable. The first condition gives the tangential mass flux, while the second specifies the normal mass flux. For

$$\psi_n = \hat{n}\cdot\nabla\psi = \frac{1}{h_1}\frac{\partial\psi}{\partial X} = -h_3(\rho v) \tag{2.48}$$

while from specifying $\psi$,

$$\frac{d\psi}{dC_1} = \left.\frac{\partial\psi}{\partial Y}\right|_{X=\text{const}} = h_2h_3(\rho u)$$

We will specify the normal mass flux across $C_1$.

Finally, we comment on the conditions along $C_2$ which is a fictitious boundary placed so that it is beyond the parabolic line. As such, no conditions should be specified along $C_2$. Far away, however, the base must look like a point source and the streamlines must be radially symmetric. For the particular case of flow from a spherical body this will be discussed in detail in section 4.2. To specify this condition in the numerical scheme should be consistent with the solution and not make the problem ill-posed.

# CHAPTER 3

## THE NUMERICAL METHOD

As we have shown in the last chapter to compute with the stream function requires the development of two algorithms. The first must be a scheme with which to solve the mixed-type equation for the stream function itself (either 2.19 or 2.22). The second is to develop an algorithm to compute the density from the stream function derivatives using either eq. (2.29) or eq. (2.22).

The solution of the mixed-type equations associated with the potential formulation is routine. Since the properties of the stream function equations are similar, the algorithms will also be similar. Differences can arise, however, in the choice of the equation and in the form of the dissipation added in the hyperbolic regions. In Section 1 we explain our choice of the quasilinear form (2.22). Next, in Section 2, we define the difference schemes for elliptic and hyperbolic regions and discuss the dissipation terms added to stabilize the latter. The discussion is completed in Section 3 where the relaxation schemes are presented.

The next part of the chapter deals with the computation of the density. We have shown in Section 2.2 the advantage of first computing the speed from the stream function and then the density. In Section 3.4 we discuss in detail the Hafez and Lovell(1981) algorithm and show that it cannot be used without modification for some

important applications. Also in Section 4 we present a simpler method that can be used for computing internal flows and, in particular, the flows which we have chosen for the applications. Finally, in section 5 the problems used to test the code that was developed are reviewed.

### 3.1 Choice of Equation

We have chosen to solve the quasilinear form of the stream function equation, eq. (2.22) and feel that it is important to promote methods based on the quasilinear form in addition to the vorticity form. Our choice depends mostly on the fact that the numerical properties of the quasilinear form will more closely mimic the properties of the second order partial differential equation which must be used for analysis. This follows because, for the relaxation schemes commonly in use, the coefficients (particularly $\rho$) must be evaluated at a previous level of iteration. For the vorticity equation, information about the type and characteristics is implicit in the frozen density values; For the quasilinear form such information is explicit. The advantage shows up in the solution of the potential equation as greater reliability of the relaxation schemes for the quasilinear form over the conservation form (Yu, Seebass and Ballhaus, 1978). Since we were testing a new formulation on problems not before solved in this manner, we felt that the need for reliability was the deciding factor.

Though we will be computing only smooth flows, supersonic flows are usually characterized by the presence of shocks. Some comment should be made about the use of the quasilinear form instead

of the conservation form in flows with shocks. The conservation form is used in the potential computations because it has the proper weak solutions. The same criteria does not necessarily apply to the stream function equations as we showed in Section 2.3. We might expect, though, that because of the jumps in the first derivatives of $\psi$, the vorticity equation will give more accurate shock jumps. Nevertheless, we make an important point about shock fitting. Because of the extra effort required to compute the density in the stream function formulation over the potential formulation, the real advantage in computing discontinuous flows is to be able to include the vorticity introduced by the entropy jump across a shock. (See Hafez and Lovell(1981) and Lin and Rubinov(1948)). To include this jump some sort of shock tracking must be made. In that case the shock might as well be fit exactly and the problem of weak solutions is side-stepped.

Finally, we write down the equation in the form we actually use in computation. Because $h_3 \to 0$ as the rotational symmetry axis is approached, we have found it is more accurate not to differentiate the $h_3$ terms. We obtain the form below by substituting for $\zeta_3$ and w from eqns. (2.28) and (2.26).

$$\begin{aligned} L &= h_2(A\psi_X)_X((\rho a)^2-(B\psi_Y)^2) + AB\psi_X\psi_Y(h_1(A\psi_X)_Y + h_2(B\psi_Y)_X) \\ &\quad + h_1(B\psi_Y)_Y((\rho a)^2 - (A\psi_X)^2) + G \end{aligned} \tag{3.1a}$$

where G represents the lower order terms

$$G = ((\rho a)^2 - (\rho Q)^2)(A\psi_X(h_2)_X) + B\psi_Y(h_1)_Y)$$
$$+ \rho^2 h_2 A\psi_X(\Phi_X - c^2(h_3)_X/h_3^3)$$
$$+ \rho^2 h_1 B\psi_Y(\Phi_Y - c^2(h_3)_Y/h_3^3) + \rho^4 a^2 J(cc'/h_3^2 - H') \qquad (3.1b)$$

## 3.2 Differencing Schemes

For computational purposes, the unbounded region $\Omega$ exterior to the flow surface $S$ described in section 2.1 is replaced by the finite region $\Omega_o$. The use of an arbitrary coordinate system $(X,Y,\phi)$ and the axisymmetry easily allows us to map $\Omega_o$ onto the rectangle $R=[0,X_o]x[0,Y_o]$. (See figure 3.1.) We discretize R by the grid

$$X = i\Delta X \qquad i = 0,1,2,\ldots,I$$
$$Y = j\Delta Y \qquad j = 0,1,2,\ldots,J$$

Furthermore, we use the freedom of the transformation to set $\Delta X = \Delta Y = 1$ so that $X_o = I$ and $Y_o = J$. The discretization of any function $F(X,Y)$ defined on R will be denoted by $F_{ij} = F(i,j)$. For any $F_{ij}$ define the difference operators

$$D_X^+ F_{ij} = F_{i+1,j} - F_{i,j}$$
$$D_X^- F_{ij} = F_{ij} - F_{i-1,j}$$
$$D_X^o F_{ij} = (F_{i+1,j} - F_{i-1,j})/2$$
$$D_X^2 F_{ij} = D_X^+ D_X^- F_{ij} = F_{i+1,j} - 2F_{ij} + F_{i-1,j}$$

Difference operators for the Y derivatives are defined similarly.

In both elliptic and hyperbolic regions the operator L is approximated with second order centered differences. Denote $L_h$ as

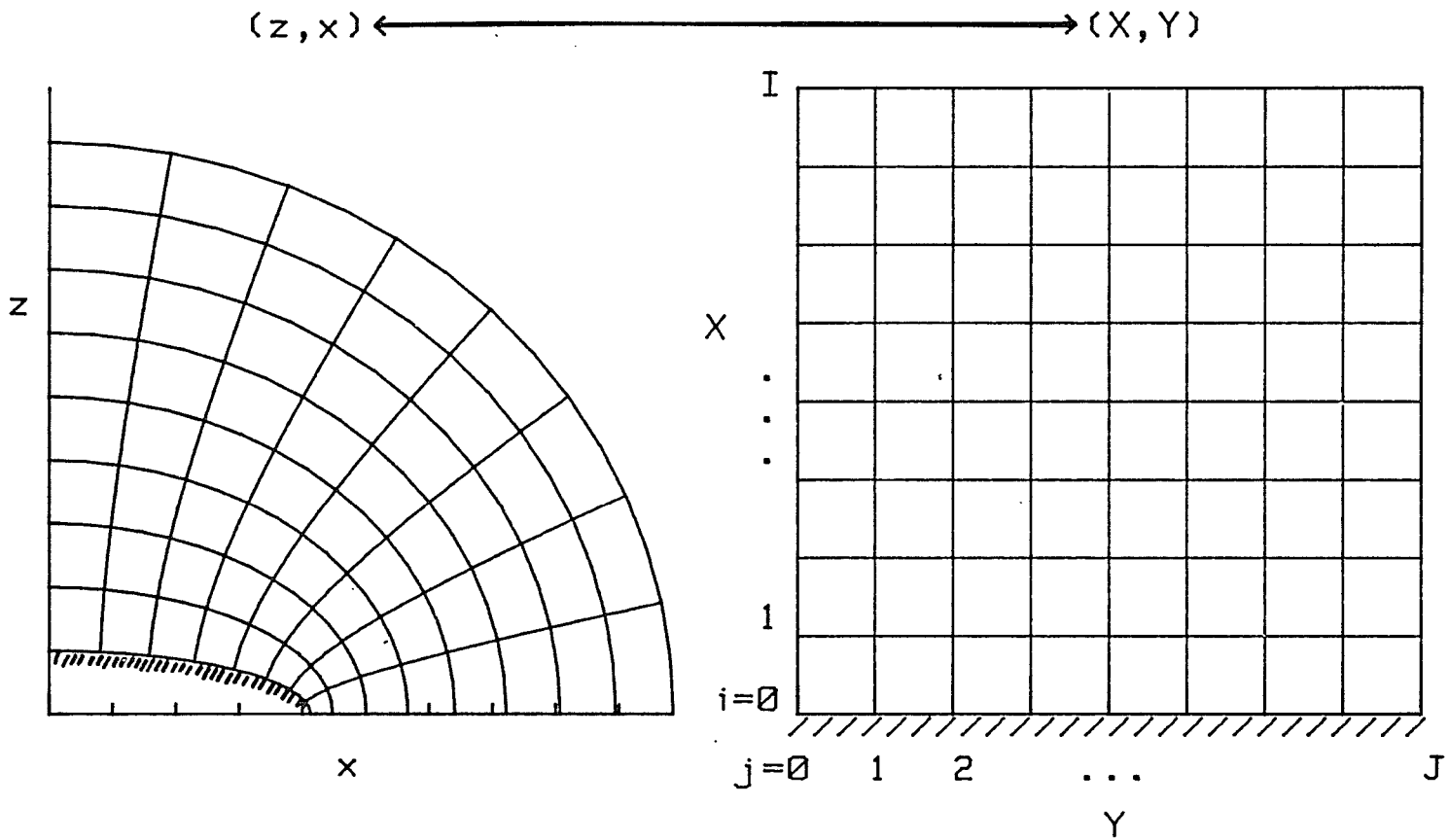


Fig. 3.1 The physical and computational domains --- The physical (z,x) space is mapped into the computational (X,Y) space through an orthogonal coordinate transformation.

the discrete operator, ignore the (i,j) subscripts, and interpret all explicit derivatives as central differences. Then

$$\begin{aligned} L_h = {} & h_2((\rho a)^2 - (B\psi_Y)^2)D_X^-(A_{i+1/2,j}D_X^+\psi) \\ & + AB\psi_X\psi_Y(h_1D_Y^o(AD_X^o\psi) + h_2D_X^o(BD_Y^o\psi)) \\ & + h_1((\rho a)^2 - (A\psi_X)^2)D_Y^-(B_{i,j+1/2}D_Y^+\psi) + G \end{aligned} \tag{3.2}$$

The derivatives of $\psi$ in the lower order terms, G, are all approximated by central differences. Though not necessary, the metric coefficients and potential are all differentiated analytically.

The difference molecule for $L_h$ appears in figure 3.2. The coefficients A and B are defined between nodes while all other quantities are evaluated at node points.

It is well known, however, that a Von Neumann analysis shows centered differences are unstable when used in a marching scheme in hyperbolic regions. To stabilize the scheme a dissipation term in the form of an artificial viscocity is added. We explicitly add to $L_h$ a first order dissipation operator based upon the rotated difference scheme of Jameson(1974).

The basic approach to adding the needed artificial dissipation is to locally rotate L to coordinate independent form. Jameson originally applied his scheme to the quasi-linear full potential equation but since the mathematical properties of the stream function equation are identical to those of the potential equation, the ideas will be the same. Let (s,n) represent the local streamwise and normal directions in an azimuthal plane. The principal part of L can be written in terms of these coordinates as

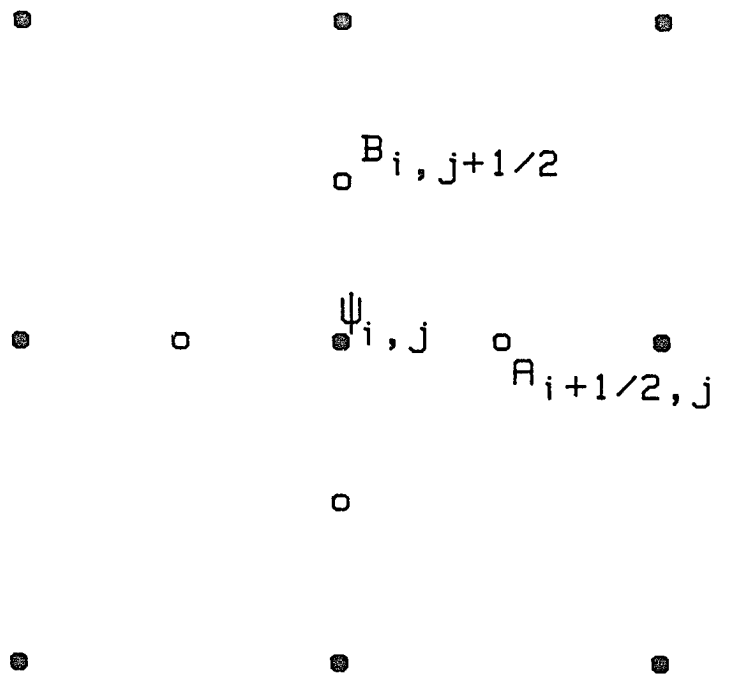


Fig 3.2 The computational molecule --- The stream function, $\psi$, is defined at mesh points (i,j). The coefficients A and B which come from the coordinate transformation are defined at half mesh values.

$$\frac{h_1 h_2 \rho^2}{h_3}((a^2 - Q^2)\psi_{ss} + a^2\psi_{nn}) \tag{3.3}$$

which is explicitly hyperbolic when $Q^2 > a^2$. If we assume the coefficients are locally constant, the streamwise and normal derivatives are related to the coordinates (X,Y) by

$$\psi_{ss} = \frac{1}{Q^2}((u/h_1)^2\psi_{XX} + 2uv/(h_1h_2)\psi_{XY} + (v/h_2)^2\psi_{YY}) \tag{3.4}$$

$$\psi_{nn} = \frac{1}{Q^2}((v/h_1)^2\psi_{XX} - 2uv/(h_1h_2)\psi_{XY} + (u/h_2)^2\psi_{YY}) \tag{3.5}$$

The idea of the rotated differencing scheme is to upwind difference the X and Y derivatives occurring in the streamwise derivative (3.4) and central difference those in (3.5). For u,v>0, the upwind approximations to the second derivatives are approximations to

$$\begin{aligned} D_X^- D_X^- \psi &\simeq \psi_{XX} - \Delta X \psi_{XXX} \\ D_Y^- D_Y^- \psi &\simeq \psi_{YY} - \Delta Y \psi_{YYY} \\ D_X^- D_Y^- \psi &\simeq \psi_{XY} - \Delta X/2 \psi_{XXY} - \Delta Y/2 \psi_{XYY} \end{aligned} \tag{3.6}$$

If the approximations of eq. (3.6) are substituted into (3.4) and eq. (3.5) and the result is then substituted into eq. (3.3), the use of rotated differencing is equivalent to explicitly adding the dissipative term

$$\frac{\mu h_1 h_2 \rho^2}{h_3}\ (\Delta X(u/h_1)^2\psi_{XXX} + uv/(h_1h_2)(\Delta X\psi_{XXY} + \Delta Y\psi_{XYY}) + \Delta Y(v/h_2)^2\psi_{YYY}) \tag{3.7}$$

to the central difference operator $L_h$ in eq. (3.7). We have defined $\mu = \max(0,1-1/M^2)$ and the derivatives are approximated by

$$\begin{aligned} \psi_{XXX} &\simeq D_X^- D_X^2 \psi \\ \psi_{YYY} &\simeq D_Y^- D_Y^2 \psi \\ \psi_{XXY} &\simeq D_Y^- D_X^2 \psi \\ \psi_{XYY} &\simeq D_X^o D_Y^2 \psi \end{aligned} \tag{3.8}$$

A similar form is derived for $u>0, v<0$ which is the only other case to consider for the applications in Chapter 4.

With the addition of the dissipation terms the treatment of the boundary conditions is not obvious. Along the mesh lines next to the symmetry boundaries the difference approximation for $\psi_{YYY}$ may require points outside the mesh. If the symmetry properties are used to eliminate the extra points the scheme is unstable. However, since the flow near the boundaries must be closely aligned with the grid, the contribution to this term will be close to zero. Therefore, near the boundaries the $\psi_{YYY}$ term is ignored.

The implementation of the outer boundary condition also requires some comment. As pointed out in section 2.6, no physical condition should be specified. The difference equations, on the other hand, require additional data. We use the zeroth order extrapolation $\psi_{I,j} = \psi_{I-1,j}$ which is an approximation to $\psi_X = 0$. Physically, this means that the streamlines are along the X coordinate lines. Since these lines are effectively radial far from the base for the problems we solve, this condition is at least consistent with the expected flow solutions (see section 4.2).

For those familiar with potential calculations, two interesting observations can be made. First, from eq. (3.3) the dissipative term effectively modifies the rotated differential equation to

$$\frac{h_1 h_2 \rho^2}{h_3}((a^2 - Q^2)\psi_{ss} + a^2\psi_{nn}) = -\nu\,\psi_{sss} \tag{3.9}$$

which is equivalent to the equation solved by the potential formulations.

Next, the form of dissipation introduced by the rotated differencing scheme has an advantage over that used in potential flow. If the flow is aligned with the grid the dissipation term eq. (3.7) is identically zero. Then the results are second order accurate even in the hyperbolic regions. Results using the potential equation will always have first order truncation errors.

### 3.3 Relaxation Method

Because the difference operators for the stream function equation look just like those for the potential equation, the same relaxation schemes can be used. We chose the successive-line overrelaxation (SLOR) method used by Jameson (1974). The SLOR method is much slower than more recent techniques (see Ballhaus et. al. 1978) but is very reliable and does not require the sensitive adjustment of a number of parameters.

Let the superscript n denote the $n^{th}$ step of the iteration process. Define the correction $C_{ij}^{n} = \psi_{ij}^{n+1} - \psi_{ij}^{n}$. The relaxation scheme can be formally written as

$$NC_{ij} + \omega L_h \psi_{ij} = 0 \tag{3.10}$$

where N determines the type of relaxation scheme and$\omega$ is a relaxation parameter. The matrix N is chosen to approximate $L_h$ yet must be simple enough to invert easily (see Ballhaus et. al.,1978). When the operator is elliptic, N is similar to that derived for Laplace's equation. We use

$$\begin{aligned}(h_2((\rho a)^2-(B\psi_Y)^2)(-A_{i+1/2,j} - D_X^{-}A_{i+1/2,j}) \\ + AB\psi_X\psi_Y(h_1 D_Y^{o}A + h_2 B_{i-1,j}T_X^{-1}D_Y^{o}) \\ + \omega h_1((\rho a)^2 - (A\psi_X)^2)(D_Y^{-}B_{i,j+1/2}D_Y^{+}))C_{ij} + \omega L_h\psi = 0\end{aligned} \tag{3.11}$$

Where $T_X^{-1}C_{ij}$ is the unit shift operator in the X direction. The operator N approximates the highest order derivatives of L. The matrix inversion problem for solving for C is NC = F which is a diagonally dominant tri-diagonal system.

For the supersonic relaxation scheme to be stable, the marching direction is chosen to correspond to the flow direction. Following Jameson(1974) the operator uses the overrelaxation parameter $\omega$ in such a way that the continuity of the representation of the Y-derivatives is maintained when the flow changes type.

When L is hyperbolic we also use an N similar to that derived by Jameson(1974) by viewing eq. (3.10) as representing a time

dependent process where $C = \psi_t \Delta t$. The rotated equation (3.3) is modified by adding time dependent terms like

$$(M^2 - 1)\psi_{ss} - \psi_{nn} + 2a\psi_{st} + 2b\psi_{nt} + c\psi_t \tag{3.12}$$

where a,b,c are coefficients whose properties must be determined. If the change of variable

$$T = t - as/(M^2 - 1) + bn \tag{3.13}$$

is made, eq. (3.12) is equivalent to

$$(M^2 - 1)\psi_{ss} - \psi_{nn} - 2(a^2/(M^2 - 1) - b^2)\psi_{TT} + c\psi_T = 0 \tag{3.14}$$

which is a telegraph equation (Courant and Hilbert, 1962). The marching direction for the steady state flow is the streamwise, s. For the pseudo-time dependent relaxation process to be consistent, we require c = 0 and

$$a^2/(M^2 - 1) - b^2 > 0 \tag{3.16}$$

For convenience, define the factors

$$R_s = (1/M^2 - 1)/(h_1 h_2 h_3{}^3)$$

$$R_n = 1/(M^2 h_3{}^3)$$

Using the above analysis as a guide, the iteration matrix we use for u,v > 0 is

$$NC_{ij} = 2R_s(\psi_Y{}^2 D_X^- - \psi_X\psi_Y(D_X^- + D_Y^-) + \psi_X{}^2 D_Y^-)C_{ij}$$

$$+ R_n( -(h_2\psi_X/h_1)^2 D_X^- + \psi_X\psi_Y/2D_Y^o T_Y^{-1} + (h_1\psi_Y/h_2)^2 D_Y^o)C_{ij} \tag{3.17}$$

A similar form is used for $v < 0$. To show how this relates to eq. (3.12), consider $D_X^- C_{ij}$ as an approximation to $\psi_{Xt}$. The other space derivatives above are similarly related to derivatives of $\psi$. The first term of (3.17) can be expressed as an approximation to

$$2R_s(\psi_Y(\psi_Y\psi_{Xt} - \psi_X\psi_{Yt}) - \psi_X(\psi_Y\psi_{Xt} - \psi_X\psi_{Yt})) \tag{3.18}$$

which in turn is equivalent to

$$-2J/h_3( M^2 - 1)/M^2( u/h_1 + v/h_2)\psi_{st} = 2a\psi_{st} \tag{3.19}$$

The second term is an approximation to

$$-J/(h_3M^2)(v/h_2)\psi_{nt} = b\psi_{nt} \tag{3.20}$$

so that the conditions of equation (3.15) is met. This choice also leads to a diagonally dominant tri-diagonal matrix system if the relaxation scheme is marched in the streamwise direction. Though we have not found it necessary, an additional $\psi_{st}$ term can be added so that the term does not vanish near the sonic line (see Jameson,1974). We allow the possibility of adding

$$-\varepsilon \frac{h_1 h_2}{h_3} \psi_{st}$$

where $\varepsilon$ is a small adjustable parameter.

## 3.4 Density Computation

As emphasized before, the computation of the density from the stream function is not straightforward. Right now, no unique method is available to compute the density from the stream function derivatives in all flow problems. We discuss below two approaches. Both involve first computing the speed and then the density from Bernoulli's equation. We begin by analyzing in detail the clever method of Hafez and Lovell(1981). For reasons given below, their method cannot be used directly for internal flows or the problems solved in Chapter 4. Thus we present a simple method that has proved suitable for the flow problems in Chapter 4.

Hafez(1979) and Hafez and Lovell(1981) use the vorticity equation (2.13) to compute one velocity component. In cartesian coordinates for irrotational flow,

$$u_y - v_x = 0 \tag{3.22}$$

The streamline slope is defined by

$$s = \frac{dy}{dx} = \frac{v}{u} = -\frac{\psi_x}{\psi_y} \tag{3.23}$$

If we substitute for v in eq. (3.22) a single first order linear partial differential equation for u is obtained

$$u_y - (su)_x = 0 \tag{3.24}$$

Along a characteristic direction, z, the equation is

$$\frac{du}{dz} = u_y - su_x = u_y\frac{dy}{dz} + u_x\frac{dx}{dz} = us_x \tag{3.24}$$

So that the slope of the characteristics is given by

$$\xi = -\frac{1}{s} = \frac{\psi_y}{\psi_x} \tag{3.25}$$

Therefore, because $\xi s = -1$ The characteristics of (3.22) run perpendicular to the streamwise direction. A well-posed boundary value problem for the computation of u requires that u is specified along some non-characteristic curve. For external flows around bodies this is very convenient (see fig. 3.3a). The boundary data can come directly from the far-field flow condition and eq. (3.22) can be marched inwards towards the body. Once the component u is computed, $v = -su$ provides the other component. Bernoulli's equation, then, directly gives $\rho$.

For internal flows and those which we discuss in the next chapter, the required boundary data are not known (see fig. 3.3b). Some method of determining the wall velocity from other considerations must be developed. The method must also be able to insert properly a shock which can originate at the boundary. Because the data is known only at the inflow, a method which can use that data is more suitable.

We propose a simple method which works in smooth flow or can be used in conjunction with shock fitting. In smooth flow Taylor's theorem is valid and the fluid speed at a particular point of the fluid can be determined numerically from that at an upstream point (X',Y') by

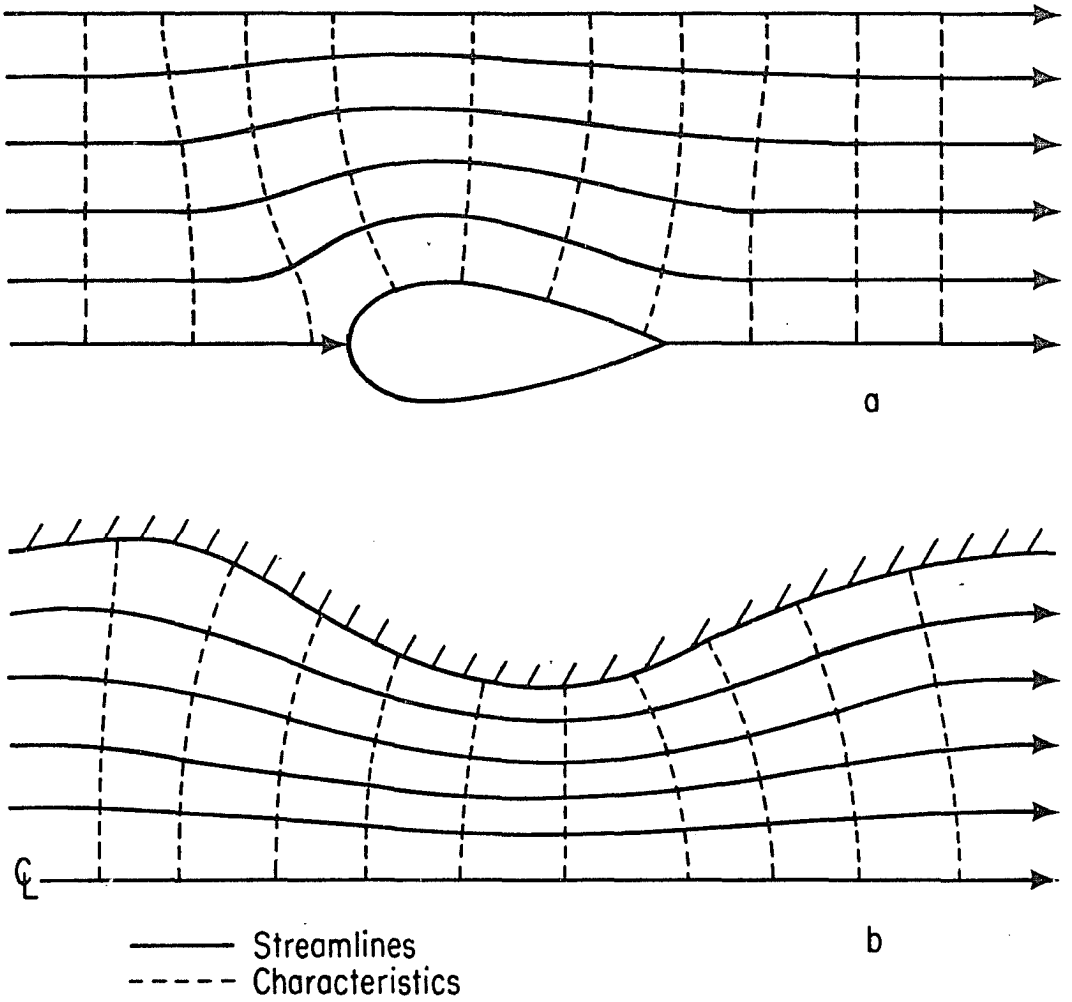


Fig. 3.3 Streamlines and the corresponding characteristics of equation (3.22) --- a) For an external flow. b) For an internal flow.

$$Q^2(X,Y) = Q^2(X',Y') + (\frac{dQ^2}{ds})ds + O(ds^2) \qquad (3.25)$$

where $dQ^2/ds = \underline{Q}/||Q||\cdot\nabla Q^2$. Effectively, the value of $Q^2$ is obtained by extrapolating from the upstream direction. This value is substituted into eqn. (2.35) to choose an approximate value, $\beta$, on the proper branch of the density function. Newton's method is then used on eq. (2.29) to get the value of $\rho$ corresponding to the actual mass flux at a given point in the following manner. Let $F(\rho)$ be the function on the right of eqn. (2.33). The proper value of $\rho$ is the zero of F on a particular branch chosen as above. Newton's method is

$$\rho^{k+1} = \rho^k - F(\rho^k)/F'(\rho^k) \qquad (3.26)$$

where

$$F'(\rho) = (\gamma-1)\rho^{(\gamma-2)} - f^2/\rho^3 = (\gamma-1)(a^2 - Q^2)/(\rho a_o^2) \qquad (3.27)$$

and k is an iteration index. At the hyperbolic point, $F' = 0$ and eqn. (3.26) cannot be used. There, however, eqn. (3.27) can be used directly to get the density exactly which is

$$\rho = (f^2/(\gamma-1))^{1/(\gamma+1)}$$

## 3.5 Test Problems

Before the results of any code can be accepted a substantial amount of testing must be done. In this section we describe some of the problems with which we tested the code based on the algorithms of this chapter. Most of the problems were derived from the one dimensional wind problems which are discussed in detail in the next

chapter. They included fully subsonic, fully supersonic and mixed wind type flows computed as one- and two-dimensional problems.

The fully subsonic cases tested the subsonic difference scheme, the corresponding relaxation scheme and the density computation algorithm. The flows were irrotational of the type shown in figures 4.2 and 4.4. They were computed in both spherical coordinates and in the oblate spheroidal coordinate system described in section 4.4 for the galactic wind problems. The latter coordinate system allowed the solution of a two-dimensional flow for which the exact solution was known. Solutions on more than one grid were computed to show that asymtotic second order convergence was achieved.

The fully supersonic problem which tested the supersonic relaxation and differencing schemes was the spherical expansion of a supersonic gas. The boundary condition at the inflow was formed by specifying the exact solution on the first two grid lines i = 0,1. The problem was solved in both spherical and oblate spheroidal coordinates.

The transonic flows are discussed in detail in sections 4.1 and 4.2. We mention here that in addition to those, the one-dimenional transonic wind problem was also solved in oblate spheroidal coordinates. A strictly two-dimensional problem is discussed in section 4.2.

All of the flows mentioned so far have been irrotational. To be sure the vorticity, H, and c were computed properly the incompressible problem discussed by Batchelor(1967, p. 545) was

solved. The problem is that of a swirling incompressible fluid in a right circular cylinder. In cylindrical coordinates $(z,r,\phi)$, the boundary conditions on $\psi$, H, and c are

$$\psi_o = ur^2/2$$
$$c = \Omega r^2$$
$$H = u^2/2 + \Omega^2 r^2$$

The exact solution is $\psi = \psi_o(r)$ and the initial condition was a perturbation of this.

The test problems, then, using spherical, oblate spheroidal and cylindrical coordinate systems have also been used to test the coordinate transformations. Thus, along with the tests of the vorticity computation, the subsonic and supersonic difference and relaxation schemes, all parts of the code have tested out satisfactorily.

# CHAPTER 4

## APPLICATIONS

We now apply the ideas of the previous chapters to a class of "wind" problems motivated by the one-dimensional solar wind theory developed by Parker(1963). The use of the stream function as described here is a new and different approach to solve the steady problem directly. It is far more informative than using the Euler equations because the effects of rotation, variation of H and the sources of vorticity are all explicit in the stream function equation. Because the problem has not been approached in this way before, the emphasis here is to explore the types and characteristics of the transonic solutions rather than to solve a particular physically applicable problem. Most important, we present rotational and irrotational solutions which exhibit behavior suggested by the equations.

In section 4.1 we describe in detail the 1-D mathematical theory of the solar wind. The extension of the solar wind to two-dimensional problems is presented in section 4.2. Computations of solar type models using the technique described in the last chapter will be presented in section 4.3. In the last section we will give examples of application to models of oblate spheroidal galaxy models where the gravitational potential is no longer spherically symmetric.

## 4.1 The Solar Wind Problem

In order to understand the results of the following sections for two-dimensional axisymmetric flows it is first necessary to understand the one-dimensional theory in detail. In particular, experience has shown that many people do not appreciate the role of Bernoulli's constant in solar wind-type flows so it is important to reiterate the basic results. A general presentation of the theory of the solar wind for polytropic gases was written by Parker(1963). Parker's analysis centered on Bernoulli's equation. In this section we will mix the approaches of Parker(1963) and Holzer and Axford(1970) and look at the differential equations and Bernoulli's equation simultaneously.

In spherically symmetric geometry, we choose the length scale $r_o$ as the base radius and the base density as $\rho_o$. The equations (2.9) reduce to

$$\begin{aligned} &\frac{d}{ds}(s^2\rho u) = 0 \\ &\frac{1}{2}\frac{d}{ds}(u^2) + \frac{a^2}{\rho}\frac{d\rho}{ds} - \frac{1}{s^2} = 0 \\ &\frac{1}{2}u^2 + \frac{a^2}{\gamma-1} - \frac{1}{s} = H \end{aligned} \tag{4.1}$$

where $s = r/r_o$, $\Phi = -1/s$, and u is the radial velocity. Bernoulli's constant is specified by the values at the base

$$H = \frac{1}{2}u_o^2 + \frac{a_o^2}{\gamma-1} - 1 \tag{4.2}$$

Two physical constraints must be posed as boundary conditions. At the base, the pressure must be high and the velocity practically zero. This represents an effectively static atmosphere ("corona") where $M << 1$. Next, as $s \to \infty$ the pressure must tend toward zero, reflecting the fact that the gas expands into a vacuum. As we will see, these conditions profoundly influence the nature of the solutions to eqns. (4.1).

Following Holzer and Axford, equations (4.1) can be rewritten as a single equation for the Mach number, M. The density derivative of the momentum equation can be eliminated using the continuity equation. Introducing the Mach number $M = u/a$ and using Bernoulli's equation to eliminate the sound speed derivative yields, for $\gamma > 1$,

$$\frac{M^2-1}{2M^2}\frac{dM^2}{ds} = \frac{1 + (\gamma-1)/2\, M^2}{H + 1/s}\left(\frac{2H}{s} - \frac{1}{2s^2}\frac{5 - 3\gamma}{\gamma - 1}\right) \tag{4.3}$$

Because of the singularity at $\gamma = 1$, the isothermal case must be treated separately. The sound speed for an isothermal flow is a constant and the differential equation for the Mach number is

$$\frac{M^2-1}{2M^2}\frac{dM^2}{ds} = \frac{1}{s}\left(2 - \frac{1}{sa^2}\right) \tag{4.4}$$

In form these equations are very much like those for a quasi 1-dimensional duct with variable area, A(s). The right hand sides of (4.3) and (4.4) correspond to the dLogA/ds term. Consequently the solutions will have properties very similar to the well known variable

area solutions. The most striking property is the possiblility of a smooth transition from subsonic to supersonic flow.

We now qualitatively analyse eqns. (4.3) and (4.4) to show the possible types of solutions. From Bernoulli's equation the solution which satifies the boundary conditions will be determined. Starting with the simpler of the two, eq. (4.4), the equation has a critical point at

$$s_c = \frac{1}{2a^2}$$

At the critical point either $dM^2/ds = 0$ or $M^2 = 1$. If $M^2 = 1$ then l'Hopital's rule is used to show that

$$\lim_{s \to s_c} \frac{dM^2}{ds} = \pm 1/(a s_c^{3/2}) \tag{4.5}$$

For $s > s_c$

$$\frac{dM^2}{ds} \begin{cases} > 0 & \text{for } M^2 > 1 \\ < 0 & \text{for } M^2 < 1 \end{cases} \tag{4.6}$$

and for $s < s_c$

$$\frac{dM^2}{ds} \begin{cases} > 0 & \text{for } M^2 < 1 \\ < 0 & \text{for } M^2 > 1 \end{cases} \tag{4.7}$$

These observations lead to the solution diagram shown in figure 4.1.

We identify five types of solutions to equation (4.4) on figure 4.1. The boundary conditions are now used to eliminate all but one.

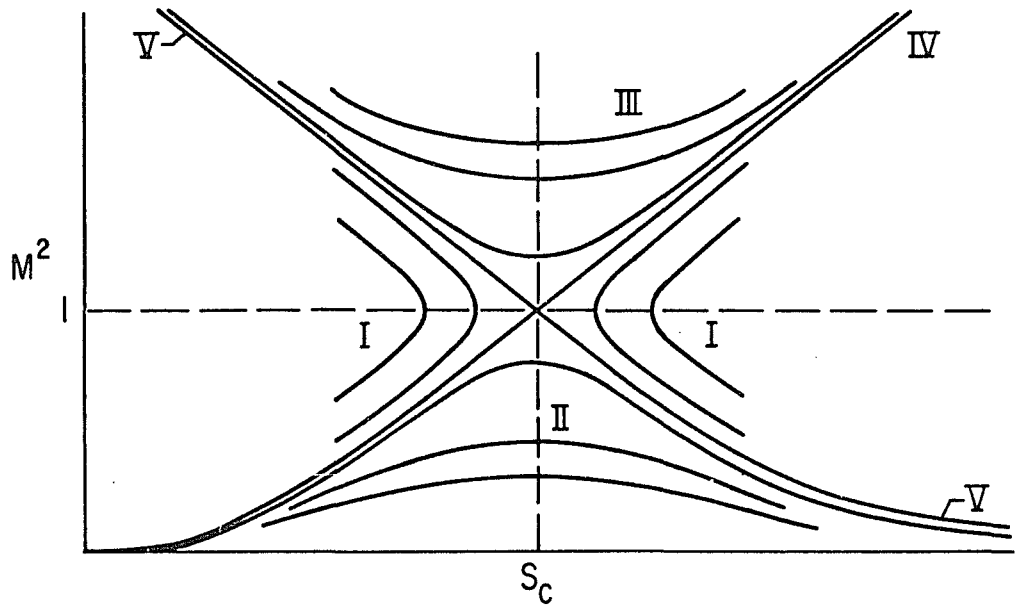


Fig. 4.1 Sketch of solutions of the spherical equations (4.3) and (4.4) --- The type IV solution which satisfies M << 1 at s = 1 and the vanishing pressure at infinity is called a "wind".

Type I solutions are double valued and are not physically possible. The type III and V solutions are eliminated because they are supersonic as $s \to 0$; They violate the boundary condition at the base. This leaves the type II and IV solutions as candidates for the solution of the boundary value problem.

Bernoulli's equation is now used to determine which of types II and IV satisfy the vanishing pressure requirement at infinity. From the continuity equation,

$$\rho = \frac{u_o}{us^2} \tag{4.8}$$

When substituted into Bernoulli's equation (2.7)

$$\frac{1}{2} M^2 - \log(u/u_o) - 2\log(s) - \frac{1}{sa^2} = \frac{H}{a^2} \tag{4.9}$$

For the type II solutions, u is small and asymtotically

$$M^2 \sim \exp(-s)\exp(-(1/s - H)) \tag{4.10}$$

Then, since

$$\rho = C\exp( H/a^2 - M^2/2 ) \tag{4.11}$$

where C is a constant,

$$\lim_{s \to \infty} \rho = C\exp( H/a^2 ) \neq 0 \tag{4.12}$$

On the other hand, $M^2 \to \infty$ on the type IV solution. Asymtotically,

$$M^2 \sim \text{sLog}(s) \tag{4.13}$$

and

$$\lim_{s\to\infty} \rho = 0 \tag{4.14}$$

Thus, the only solution which satisfies the boundary conditions is the transonic flow type IV. Following Parker, such a flow is called a "wind".

Equation (4.3) gives the behavior of the flow for $\gamma > 1$. The most important difference between the solutions of (4.3) and (4.4) is that the character of the flow depends upon H. If $H < 0$, then equation (4.3) has no critical point and the flow is gravitationally bound. Both the pressure and velocity must vanish at infinity, for if not,

$$\frac{1}{2} u^2 + \frac{a^2}{\gamma-1} < 0 \tag{4.15}$$

as $s \to \infty$. At the sun, the pressure is so large that this is not the case. The case $H = 0$ was proposed by Chamberlain(1960) as a possible model for the solar coronal expansion. If $H = 0$, there is no critical point, $dM^2/ds$ is monotonic, and the flow stays subsonic.

Equation (4.3) does have a critical point and hence has solutions resembling those of eq. (4.4) if the following conditions hold:

i) $H > 0$

ii) $\gamma < 5/3$

iii) $\frac{5 - 3\gamma}{4H(\gamma-1)} > 1$

The critical point occurs at

$$s_c = \frac{5 - 3\gamma}{4H(\gamma-1)}$$

so that the third condition merely states that the critical point must occur beyond the base.

For $H > 0$ the choice of solutions again depends on the boundary conditions and the only acceptable solution is the transonic one. If $\rho$ in eqn. (2.6) is substituted for by eqn. (4.8) Bernoulli's equation for $\gamma > 1$ becomes

$$\frac{1}{2} u^2 + \frac{a_o^2}{\gamma-1} \frac{u_o \rho^{\gamma-1}}{us^2} - \frac{1}{s} = H \qquad (4.16)$$

On the supersonic branch u is large and for large s the $u^2$ term and the $-1/s$ term balance. So, on that branch

$$\frac{1}{2} u^2 \sim H + \frac{1}{s} \qquad (4.17)$$

which is effectively constant for large s and $\rho \to 0$ as $s \to \infty$. On the subsonic branch, however, u is small and thus

$$u \sim u_o/(s^2(H + 1/s)^{\gamma-1}) \qquad (4.18)$$

so $u \to 0$ for large s and $\rho \to$ constant $\neq 0$. Thus, for $\gamma > 1$ we only accept the transonic solution.

For polytropic flow where $\gamma > 1$, then, we have shown that it is the value of H which must be specified if there is to be a wind. The isothermal results are misleading because in that case there is no restriction on H.

Because of the singularity at the sonic point equation (4.3) it is practically impossible to solve as an initial value problem starting at the base. The problem is ill-posed in the sense that small perturbations of the mass flux can cause large variations in the solution. Since the critical point is known the only effective way to solve for $M^2$ is to start there and integrate in both directions. Bernoulli's equation, on the other hand, is not singular. It is possible to specify the parameters at the base and solve for the density following the procedure outlined in section 3.4. For a given set of parameters one must allow for the existence of an expansion shock at the critical point. The proper solution can then be obtained by varying the parameters until the expansion is smooth across the critical point. It does not appear that the first approach has an analogy in multi-dimensions; The second does. Once the streamlines are known, the approach in multidimensions is identical. The parameters at the base are then adjusted until the sonic transition is smooth.

We now give an example of a solution to a particular solar wind model. The parameters $H = .75$, $\gamma = 1.1$ are chosen so the critical point is at $s_c = 5.667$. The quantity $P_0$ was chosen to give a small value of the mach number at the base. The mass flux was then changed until a smooth transonic profile was obtained. Figure 4.2 shows the types of solutions as the mass flux is increased. Figure 4.3 shows the wind solution for these parameters. Note particularly

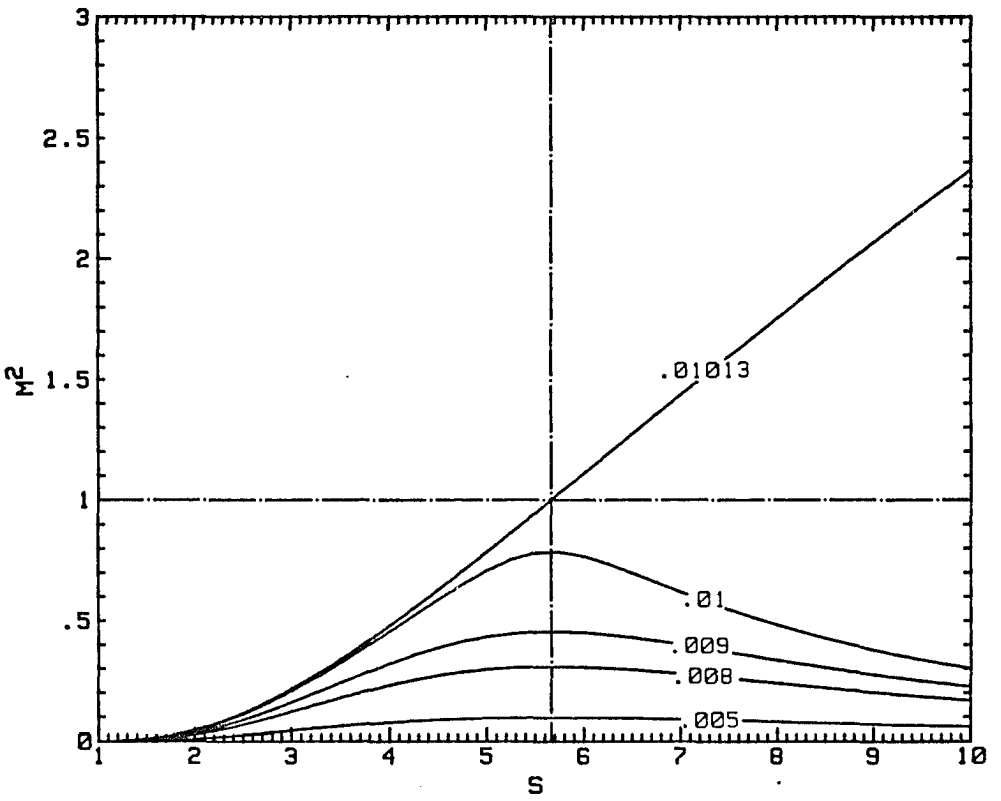


Fig. 4.2 Solutions of eqn. (4.4) for five mass fluxes --- To compute the wind solution, the mass flux is raised until a smooth transonic flow is found.

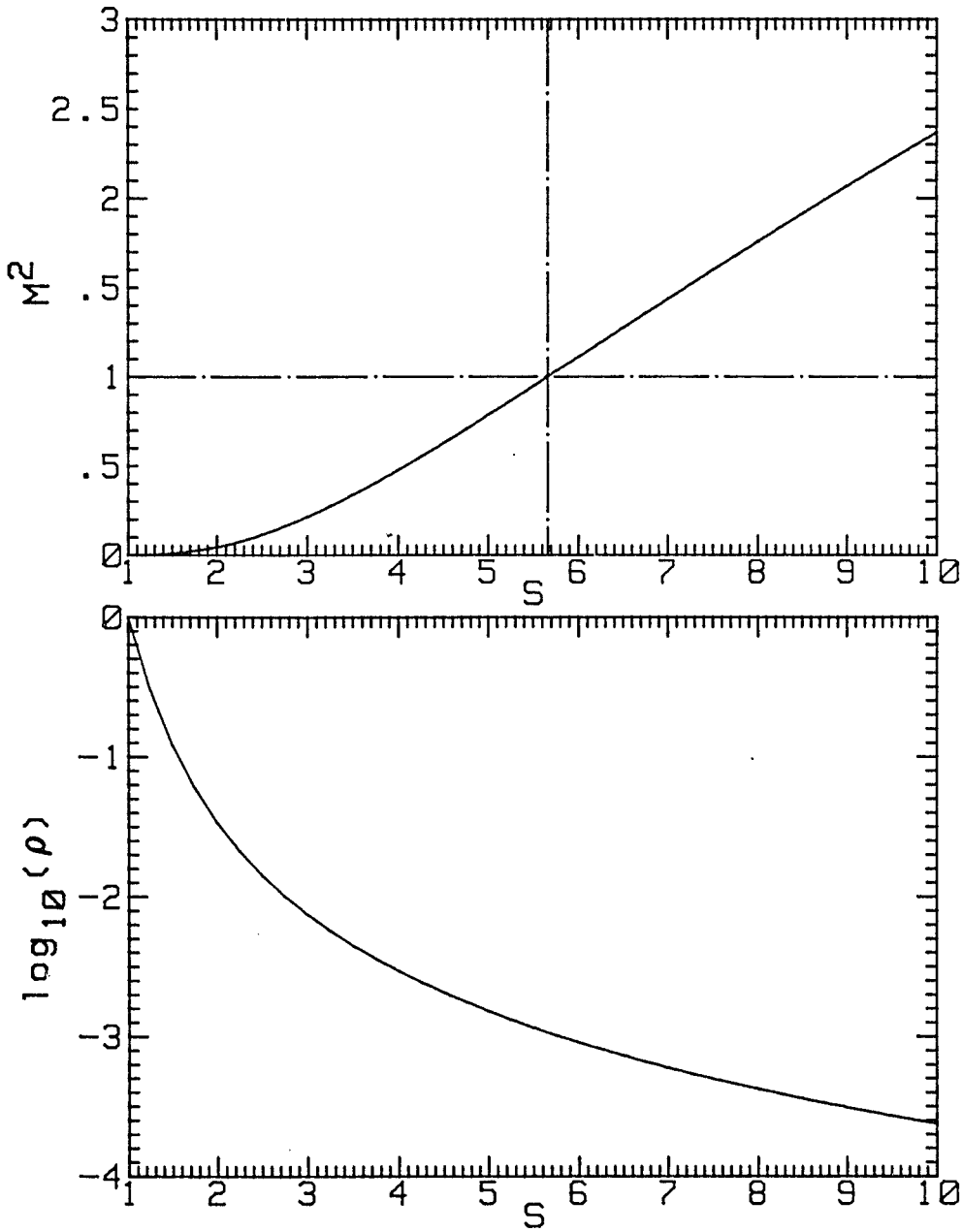


Fig. 4.3 Mach numbers and densities for a spherical wind problem --- The solution corresponds to H = .75,$\gamma$ = 1.1. Note the rapid drop in density near the base.

that while the mach number changes slowly near the base, the density drops rapidly at a rate near $s^{-2.2}$.

## 4.2 Extension to 2-D Axisymmetric Flows

Now we present the major thrust of our use of the stream function. The results of chapter 2 can be used to reformulate the one-dimensional problem discussed in the last section. In terms of the stream function we can note several features of the general wind problem not evident in the Euler equations (2.1) - (2.3). We point out these features here and in the next section present sample solutions which show them. Throughout this section we will work in a fixed spherical coordinate system $(s,\theta,\phi)$ where, as before, $s = r/r_o$ is the radial coordinate, $\theta$ is the latitude and $\phi$ is the azimuthal angle.

Suppose that the sun rotates as a solid body with angular frequency $\Omega$ and that the gas which is ejected rotates with the surface. Then the angular velocity is $w = \Omega\cos(\theta)$. Thus, from eqn. (2.26) $c(\psi)$ is known. Suppose also that H is specified at the base so that $H(\psi)$ is known. Computationally, these functions are represented with a cubic spline of the values at the base. The stream function equation in this case is

$$(a^2 - u^2)\psi_{ss} - \frac{2uv\psi_{s\theta}}{s} + \frac{(a^2 - v^2)\,\psi_{\theta\theta}}{s^2} \tag{4.19}$$

$$+ \rho v\cos(\theta)(2u^2 + v^2) + \rho u a^2 \sin(\theta)$$

$$+ \rho\cos(\theta)\left\{u\left[\frac{c^2\sin(\theta)}{s^2\cos^3(\theta)}\right] - v\left[\frac{1}{s} - \frac{c^2}{s^2\cos^2(\theta)}\right]\right\}$$

$$+ (\rho a)^2(cc' - s^2\cos^2(\theta)H') = 0$$

The vorticity is

$$\zeta_3 = -\rho\left[H's\cos(\theta) - \frac{cc'}{s\cos(\theta)}\right] \tag{4.20}$$

This is a much more informative form than the Euler equations, (2.9), for without solving these equations some interesting qualitative results can be obtained. We see that the effect of rotation is two-fold. First, the rotation modifies the gravity field. The effective radial gravitational force becomes

$$g_s = \frac{1}{s^2}\left[1 - \frac{c^2}{s\cos^2(\theta)}\right] \tag{4.21}$$

while an effective latitudinal force is introduced

$$g_\theta = -\frac{c^2\sin(\theta)}{s^2\cos^3(\theta)} \tag{4.22}$$

In addition to modifying the gravity field, the rotation introduces vorticity. The contribution from the rotation is

$$\zeta_{rot} = \frac{\rho cc'}{s\cos(\theta)} \tag{4.23}$$

The most interesting fact here is that this contribution to the vorticity lies only in a small "boundary layer" beyond the base. To prove this, remember that both c and c' are specified along the boundary and hence are bounded by the maximum and minimum values there. In the last section we indicated that the density drops as $s^{-2.2}$. Thus, the vorticity must drop rapidly as $s^{-3.2}$. This is much slower than the decay in viscous boundary layers at a wall, nevertheless the vorticity drops off on a scale much smaller than, say, the distance to the sonic surface.

The effect of Bernoulli's function in determining the position of the streamlines is also two-fold. First, its magnitude along a streamline determines the coefficients $\rho$ and $a^2$. It also introduces a vorticity. The rate of decay, however, is much less than that due to rotation; the vorticity drops as $s^{-1.2}$. An interesting consequence is that the vorticity may change sign within the boundary layer determined by $s^{-1.2}$ depending on the magnitude of $H'(\psi)$ and $c(\psi)$.

Finally, the condition of radial flow at infinity is consistent with this the behavior of the vorticity. Far from the base the irrotational solution is just the spherically symmetric radial flow. To see this, examine the limit of eqn. (4.19) as $s \to \infty$. Through Bernoulli's equation u and v are bounded and $\rho \to 0$. The stream function will be smooth so its derivatives are bounded. Then the only remaining term far from the base is

$$(a^2 - u^2)\,\psi_{ss} = 0$$

$$\Rightarrow \psi_{ss} = 0 \Rightarrow \psi_s = \text{constant in } \theta$$

Since the symmetry boundaries are streamlines, $\psi_s = 0$ so that far from the base it is zero everywhere and the streamlines are effectively radial. This result also shows that it is difficult to infer the conditions at the base from the properties of the flow far from the base. In the next section we will present examples of the behavior derived qualitatively from eqn. (4.19).

## 4.3 Solar Wind Type Solutions

Now that basic properties of wind solutions have been discussed we show solutions obtained from the algorithm described in chapter 3. This section not only provides examples of solutions but also examines the behavior of the numerical scheme. We will study radial, two-dimensional irrotational and two-dimensional rotational cases.

### Radial Flow

To start, the example of section 4.1 is solved with the two-dimensional code for $\psi$. It is easy to see that for H = constant and c = 0 the solution to eqn. (4.19) is $\psi = \rho u \sin(\theta)$ where $\rho u$ is the normal mass flux. The solution shown in fig. 4.4 was computed with a 16x16 point grid with an initial guess

$$\psi = \rho u \sin(\theta)\left(1 - \varepsilon \sum_{n=1}^{15} \left(\frac{\cos((2n-1)\theta)}{2(2n-1)} + \frac{\cos((2n+1)\theta)}{2(2n+1)}\right) \sum_{m=1}^{15} \sin(\pi m i / I)\right) \quad (4.24)$$

where $\varepsilon$ was chosen to be 0.2. Not too much latitude is possible in the choice of an initial guess. From figure 2.2, remember, if the gradient of $\psi$ is too large there are not values of $\rho$ which satisfy

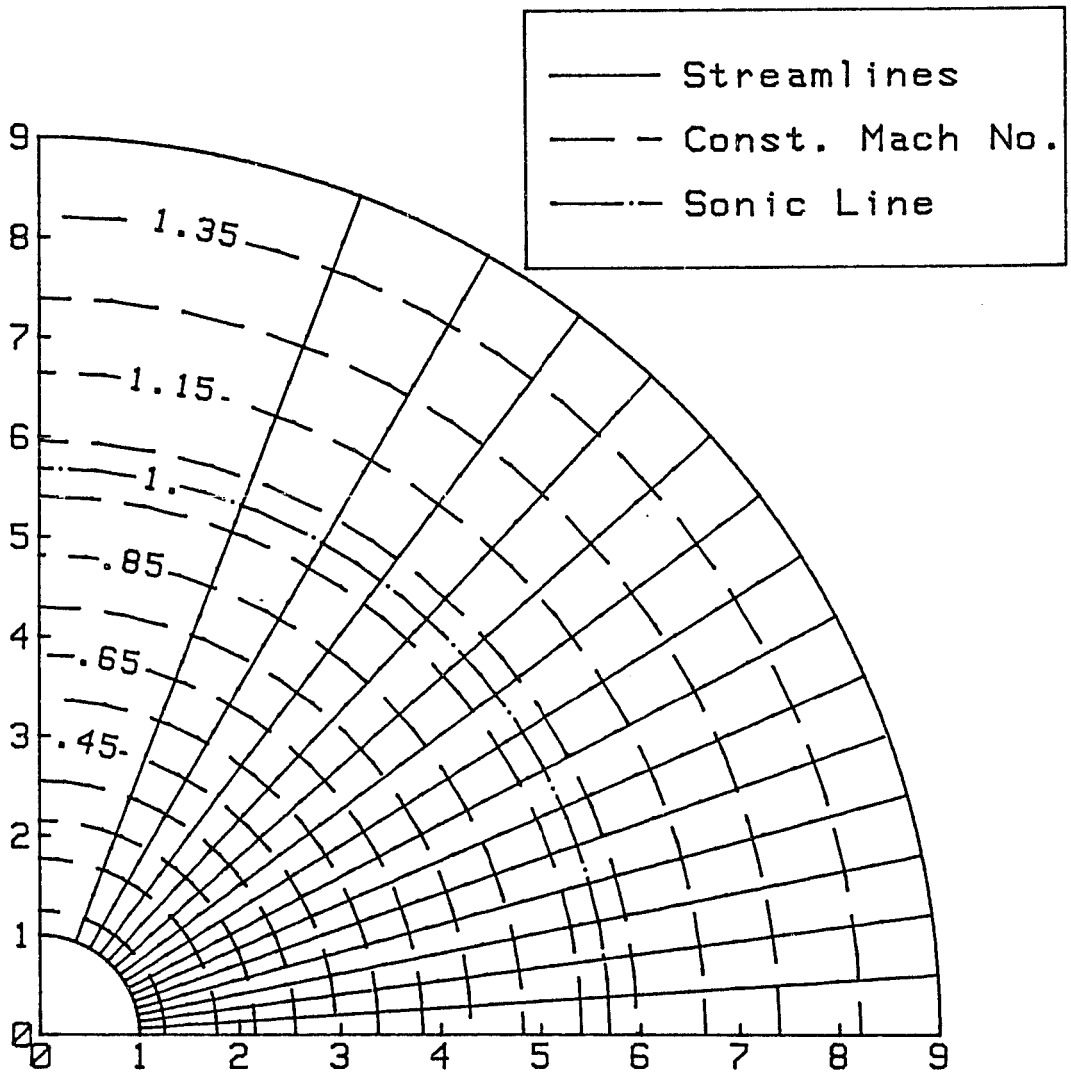


Fig. 4.4 The spherically symmetric solar wind example of fig. 4.3 solved with the two-dimensional code for $\psi$ --- The circle s = 1 corresponds to the base through which the gas flows outward along the streamlines.

Bernoulli's equation. Also, for the relaxation scheme to be stable the component u must be positive. The choice of eqn. (4.24) includes all the frequency information on the mesh yet satisfies these requirements.

On figure 4.5 are plotted the absolute percentage errors of the computed solution taken along a streamline of fig. 4.4 from the solution shown in fig. 4.3. It is not surprising that the largest errors occur at the sonic point. The results probably indicate a small expansion shock could still exist in the solution. An advantage in accuracy of using the stream function can also be seen in fig. 4.4b. Because the density is computed from an algebraic relationship, even though the mesh interval is $\Delta s = 0.5$ the density is accurate to less than 0.05% in the region near $s = 1$.

Figures 4.6 - 4.8 show the convergence behavior for the algorithm for a linear, and elliptic, and a mixed spherical problem. The linear problem is that of the previous example with the density fixed at a high value so that the Mach numbers were less than 0.01. The non-linear elliptic problem is that of the $\rho u = .009$ curve of fig. 4.2. Finally, the mixed problem is that of the transonic flow shown in figures 4.4 and 4.5. Figure 4.6 shows the convergence of the linear problem for three values of the over-relaxation parameter, $\omega$. The convergence is measured in terms of the root-mean-square residual which is related to the discrete $L^2$ norm. The curves show the characteristic "knee" and leveling off of convergence rate after the high frequency errors are eliminated.

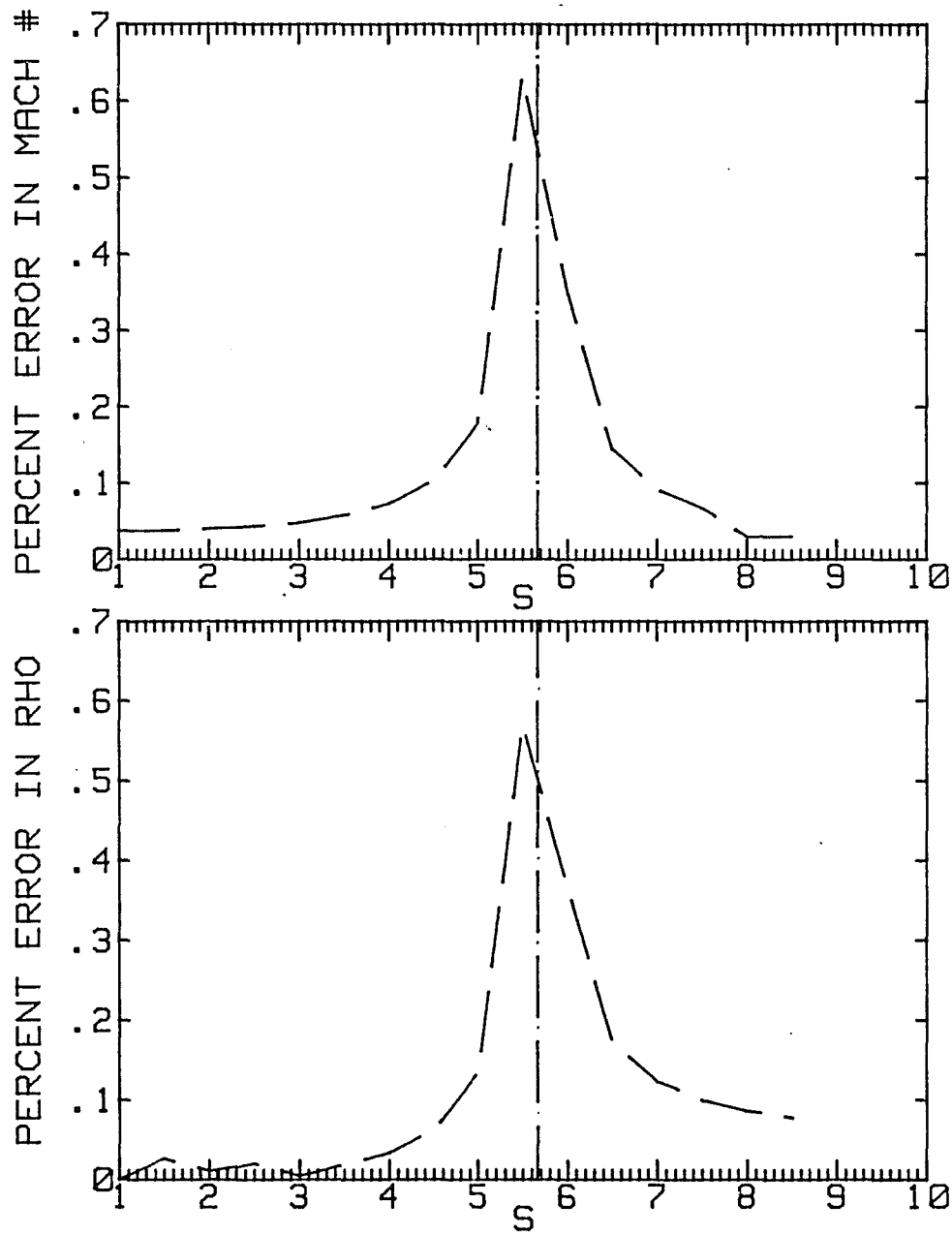


Fig. 4.5 Absolute percentage errors in Mach number and density along a streamline of the solution of fig. 4.4 --- The position of the sonic point at s = 5.667 is marked with the vertical line.

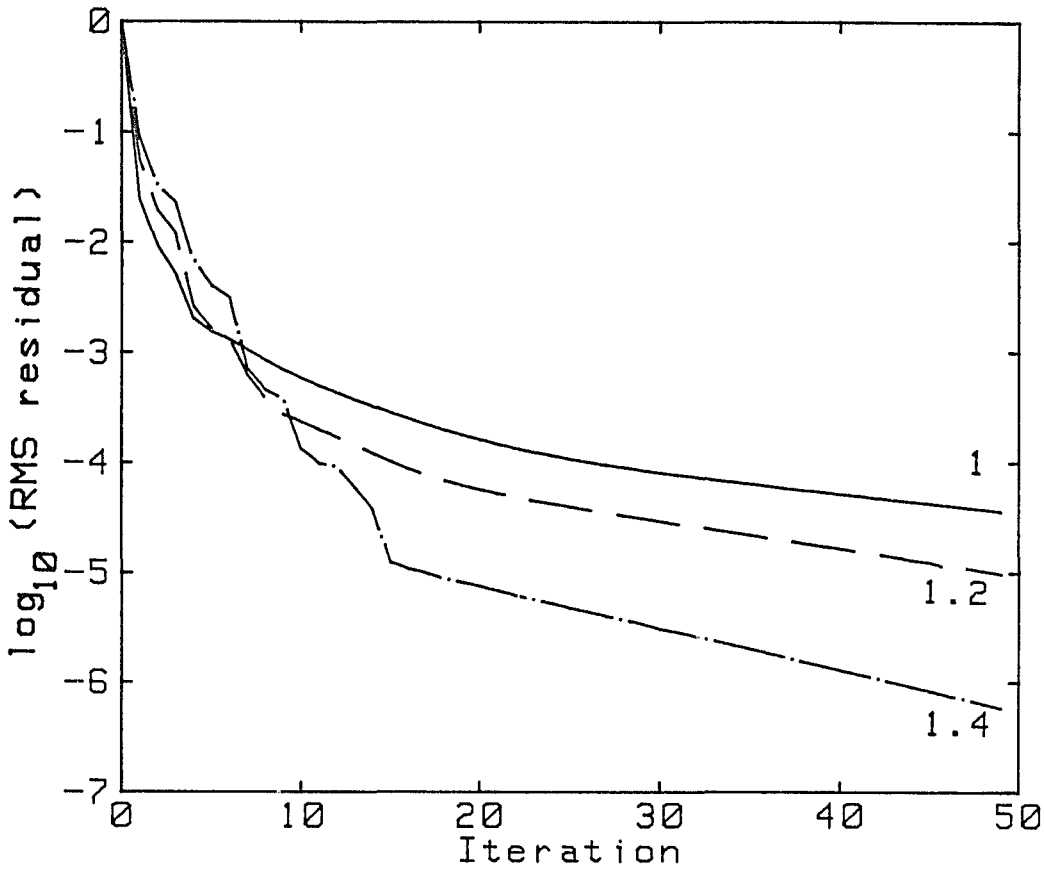


Fig. 4.6 Convergence history for the linear elliptic problem --- The problem is effectively the solution of Laplace's equation in spherical coordinates formed by a low Mach number limit of the stream function equation. Convergence behavior for three values of the relaxation parameter $\omega$ is shown.

The convergence behavior for a non-linear elliptic problem is shown in fig. 4.7. The convergence rate is oscillatory and the oscillations continue longer as the solution is over-relaxed more and more. For the non-linear problems remember that the density is also solved by an iterative procedure. How tightly the density is converged will affect the convergence behavior of the stream function too. We have used a convergence criterion on $\rho$of $\Delta\rho/\rho = 10^{-4}$

Finally, the convergence histories in figure 4.8 are for the transonic solution shown in figures 4.4 and 4.5 with the initial condition eqn. (4.24). For the transonic flows two criteria must be used to judge convergence. In addition to the RMS residual, the number of supersonic points must be monitored. For irrotational flows we find that a constant number of supersonic points is quickly established on the coarse meshes. The behavior of the residual is quite different than that for the purely subsonic and linear problems but similar to mixed flow convergence behaviors shown by Ballhaus et. al. (1978). The fact that the convergence is not accelerated greatly by varying $\omega$is probably because for these problems the subsonic region is small and the convergence rate is determined by the behavior in the supersonic zones which are not over-relaxed.

Two-dimensional Irrotational Solutions

For a special class of irrotational two-dimensional problems we can easily find the angular behavior to study the code in more than one dimension. Thus we can study the behavior of varying the mass flux along the inflow boundary and test the code at the same time.

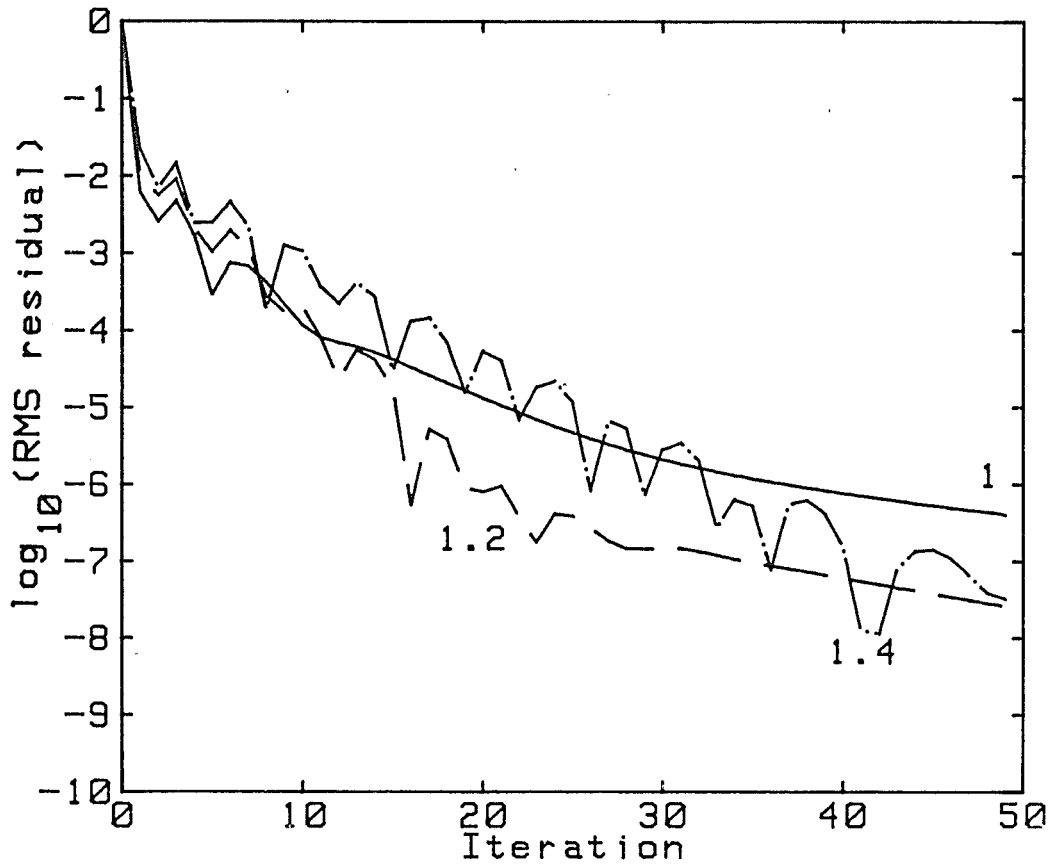


Fig. 4.7 Convergence history for the nonlinear subsonic problem --- The subsonic problem is that of the spherically symmetric $\rho u = .009$ solution shown in fig. 4.2 solved with the stream function code. Behavior for three values of $\omega$ is shown.

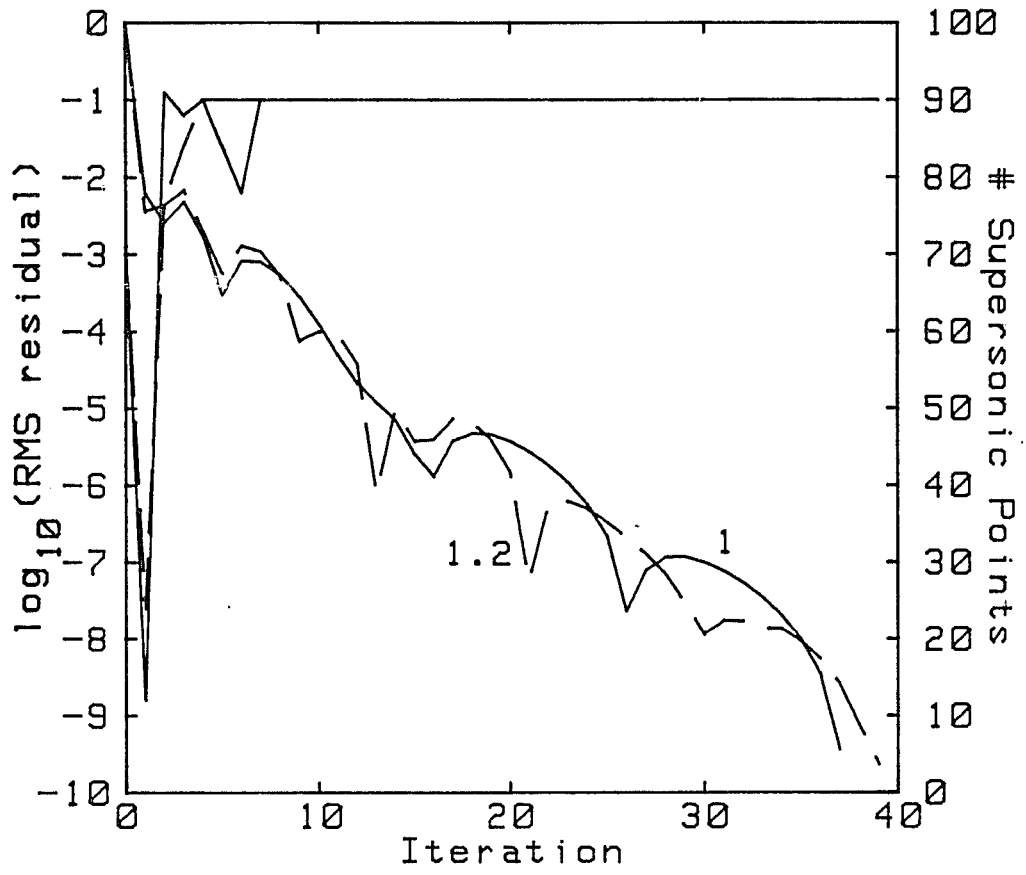


Fig. 4.8 Convergence history of the mixed flow wind problem --- The wind problem is that of fig. 4.3 with initial guess of eqn. (4.24). The number of supersonic points rapidly rises to a fixed value. The convergence for the two values of $\omega$ is quite similar.

It turns out that if the velocities u and v are represented by

$$u = a(s) + b(s)\cos(2\theta)$$
$$v = g(s)\sin(2\theta) \tag{4.25}$$

the problem is separable. For the vorticity equation in spherical coordinates is

$$\frac{\partial(sv)}{\partial s} = \frac{\partial u}{\partial \theta} \tag{4.26}$$

The functions in eq. (4.25) satisfy (4.26) provided that

$$g(s) + sg'(s) = -b(s) \tag{4.27}$$

With figures 4.9 - 4.11 we show the irrotational transonic flow from a sphere with the physical boundary condition

$$\rho u = C(1 + e\cos(2\theta)) \tag{4.28}$$

where C and e are constants. The boundary condition is that the mass flux is higher at the equator than at the pole. This corresponds to a boundary condition on $\psi$ of

$$\psi = C(\sin(\theta)(1 + e/2) + e/6\sin(2\theta)) \tag{4.29}$$

Notice that the streamlines bend more and more away from the regions of higher mass flux as e is increased. The angular variations of u and v for the e = .4 case are shown in figure 4.12 normalized to remove the radial variations. Plotted with the computed values are the exact relations of eqn. (4.25). The agreement is excellent.

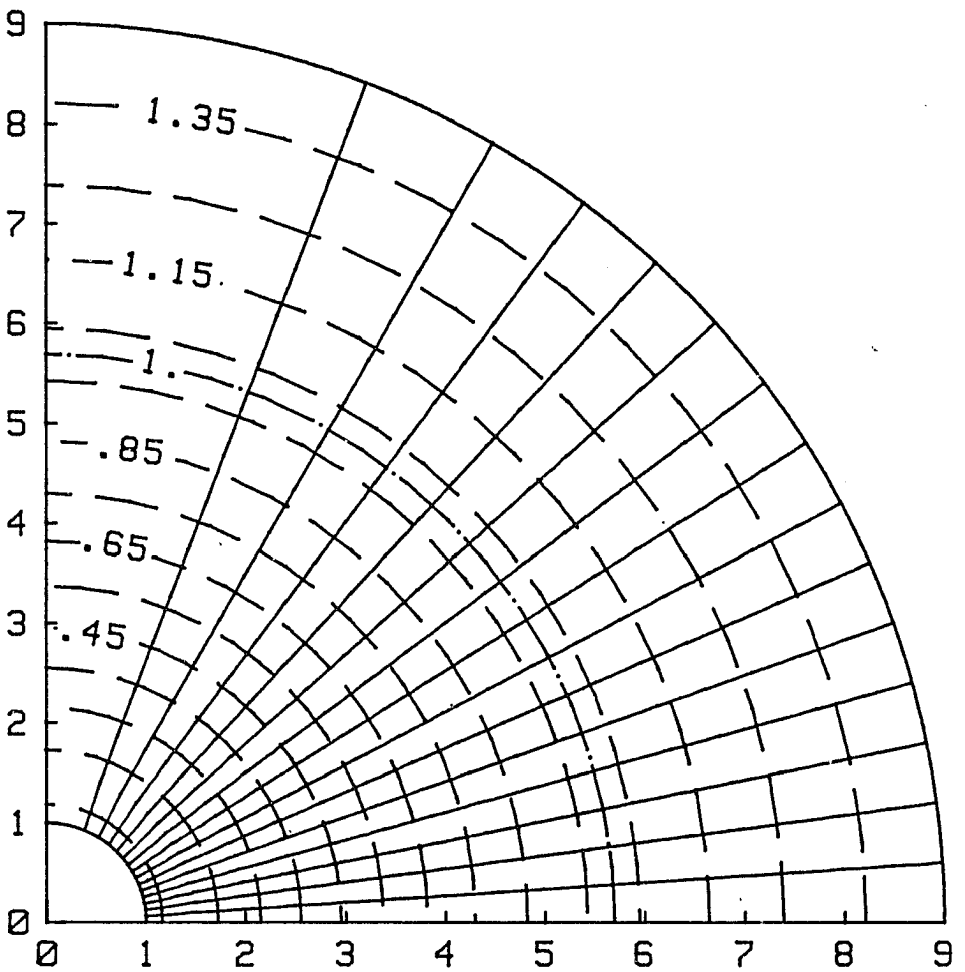


Fig. 4.9 Irrotational wind with a 10% variation in the normal mass flux --- The normal mass flux which varies from equator to pole as $\rho u \propto 1 + .1\cos(2\theta)$ has a very small effect on the wind flow.

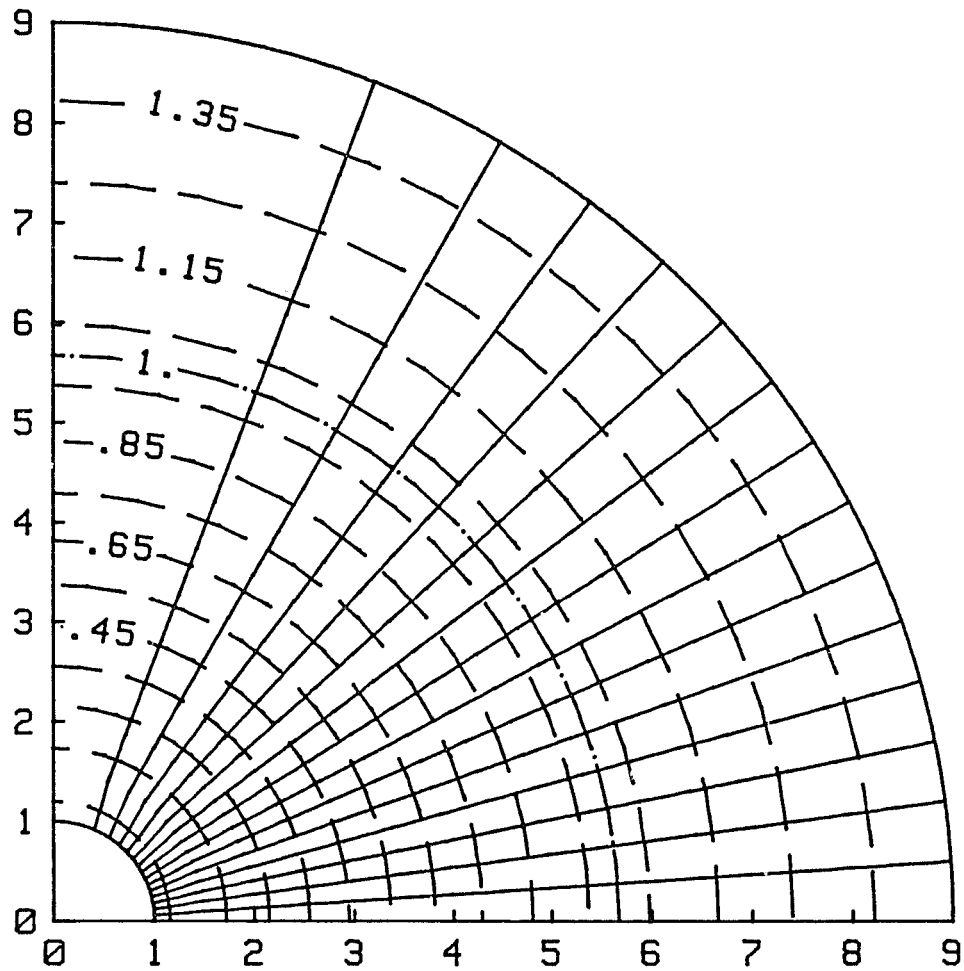


Fig. 4.10 Irrotational wind with a 20% variation of the normal mass flux --- The normal mass flux varies as in fig. 4.9. The flow is bent toward the pole and away from the region of highest mass flux.

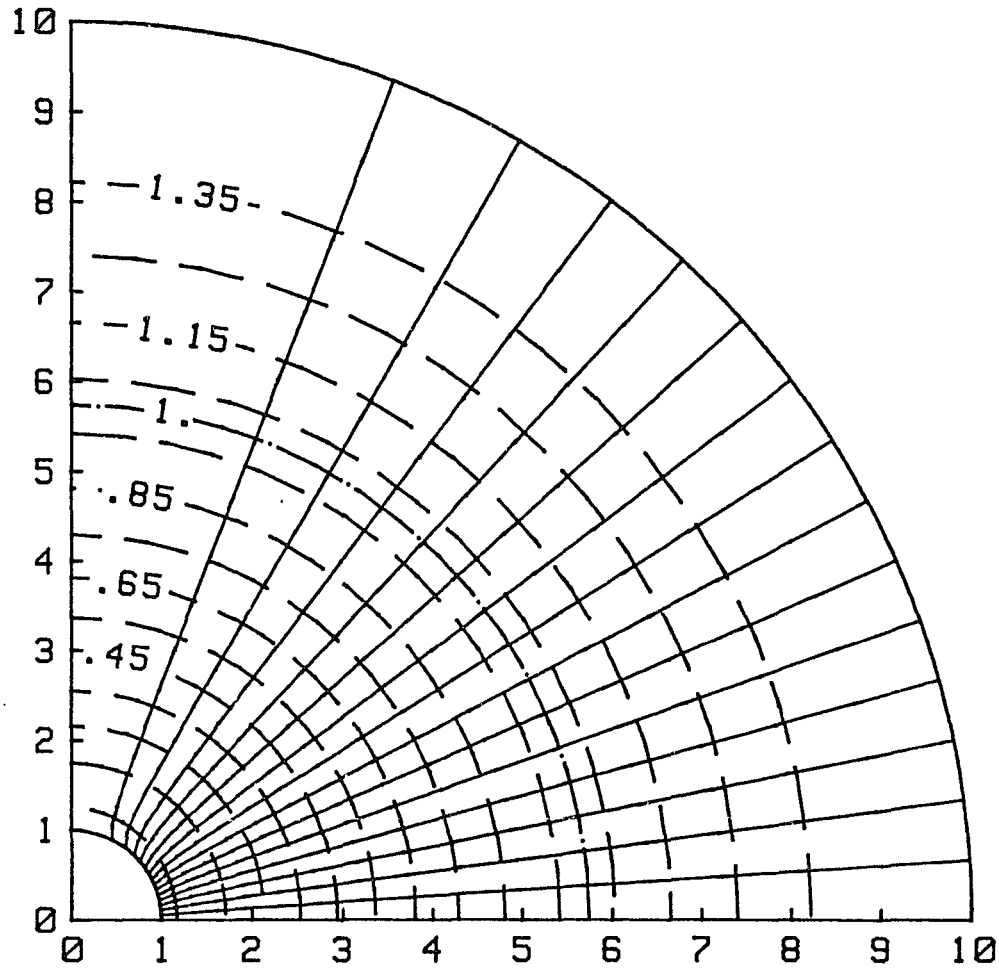


Fig. 4.11 Irrotational wind with a 40% variation in the normal mass flux --- The flow is bent strongly toward the pole but quickly straightens to the spherically symmetric solution.

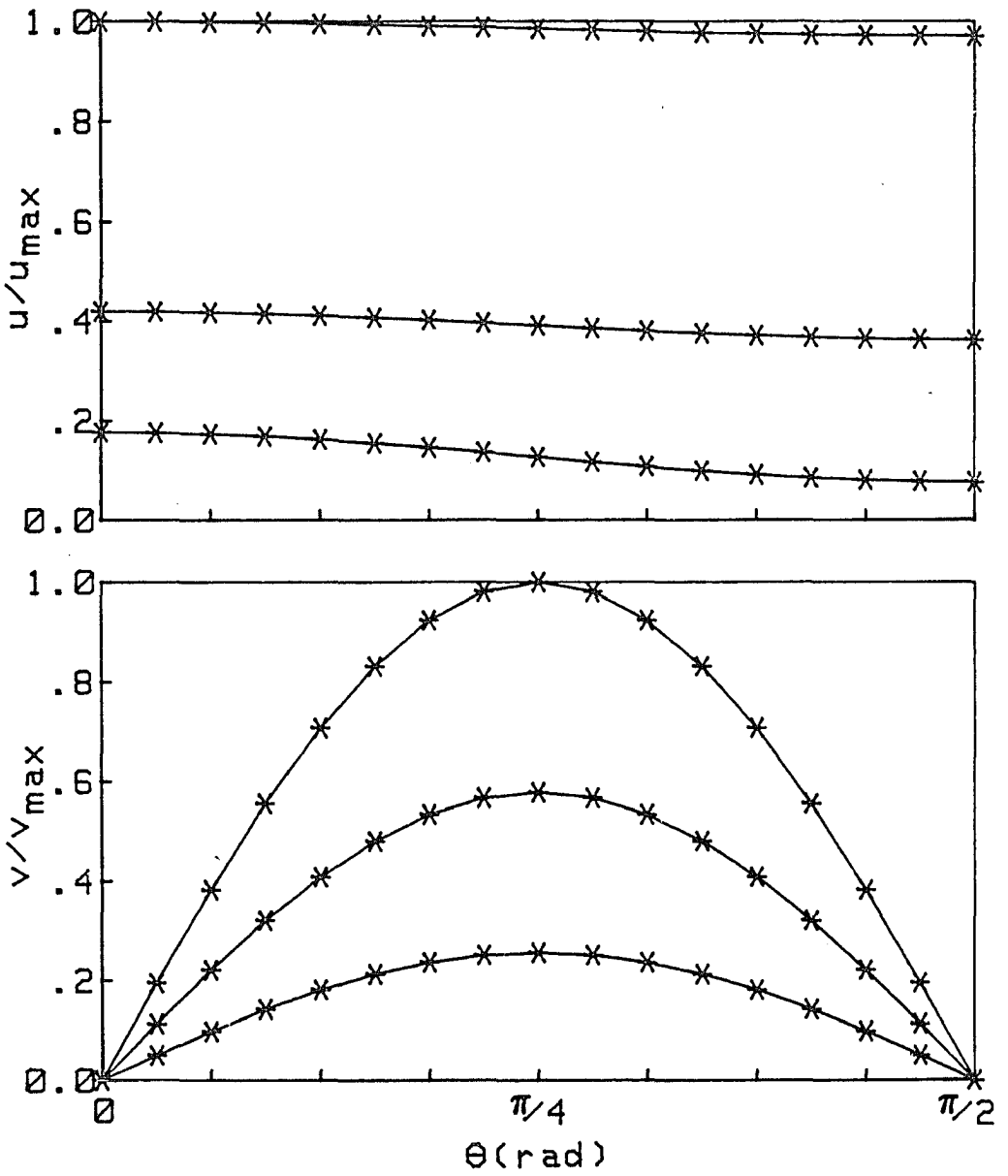


Fig. 4.12 Angular variations of the velocity for the solution of fig. 4.11 --- The exact relations given by eqns. (4.25) have been normalized to the maxima of the computed values of u and v to remove the radial variations and are represented by solid lines. The computed values are represented by *'s.

The initial values for the stream function for the two-dimensional irrotational solutions were formed by setting $\psi$ = constant along lines of constant $\theta$. The convergence behavior for these three cases is shown in fig. 4.13. The e = .4 solution was computed on a stretched mesh which concentrated the points near the base. This explains the difference in the number of supersonic points. The rapid rise of the number of supersonic points to a constant value is characteristic of the irrotational flows that we have computed.

The convergence behavior is also dependent upon the mass flux chosen. As discussed in section 4.1 the wind problem is ill-posed and numerically the sonic line can be crossed if a small expansion shock corresponding to a jump from the subsonic to supersonic branches is allowed between two mesh points. With such a jump the convergence rate suffers. We have found that the frequency of the oscillations of the residuals increases and the convergence rate slows as the expansion shock grows; the best convergence behavior occurs when the solution is smoothest. Since "smooth" is a subjective quantity this fact helps to determine how close the mass flux is to its correct value. For two dimensional flows the fact that the discretization errors will not in general be uniform means that it is difficult to get a uniformly smooth sonic transition. Thus, even the "best" choice of parameters may not give the best convergence rate. The curves on figure 4.13 for e = .4 show this effect.

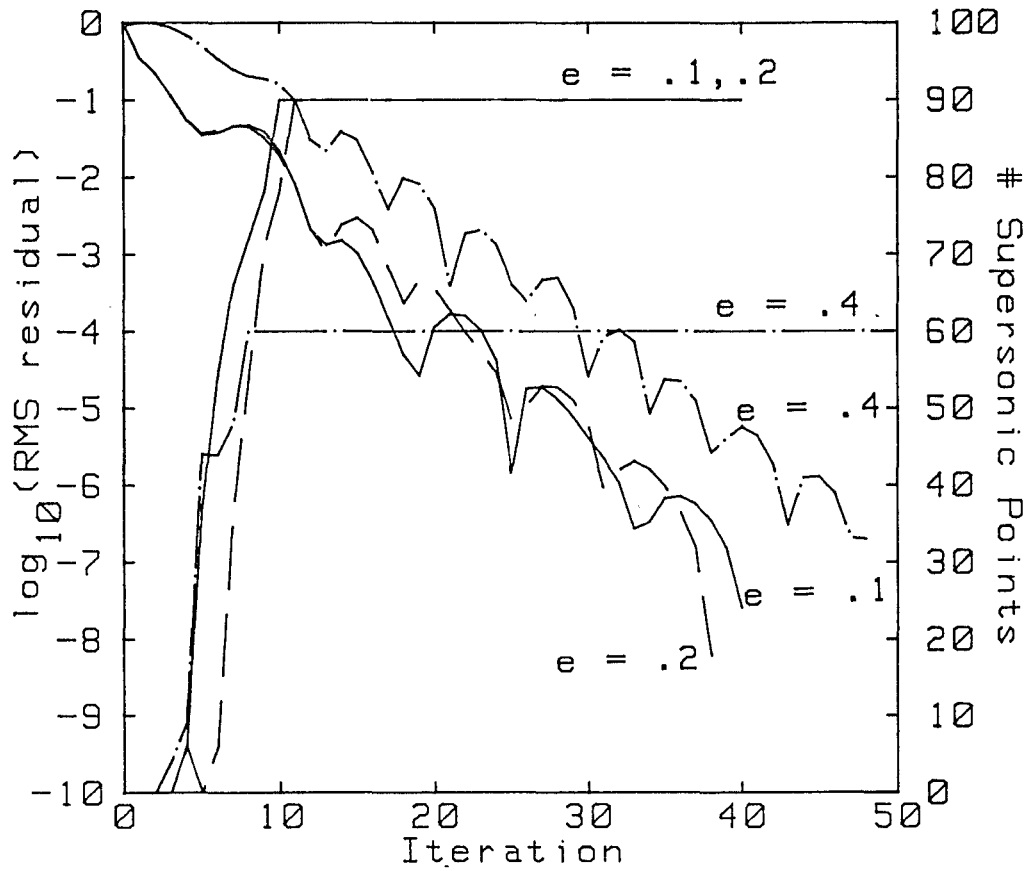


Fig. 4.13 The convergence histories for the irrotational flows with varying mass fluxes --- Shown are the residual behavior and the number of supersonic points for the solutions shown in figs. 9 - 11. The supersonic zone sets up quickly for these problems. The e = .4 case was computed on a stretched mesh which concentrated points near the base. This accounts for the difference in the number of supersonic points and the rate of convergence.

Two-dimensional Rotational Solutions

The reason for using the stream function was to be able to compute rotational flows. We now give examples of such solutions. As expected from the discussion of the last section, the effects of vorticity should occur within a small region beyond the base. Beyond that region the solution should look very similar to the spherically symmetric one.

The type of solution we show is that of a "star" which rotates as a solid body. We use a uniform normal mass flux across the base just as in the spherically symmetric problem. Bernoulli's function is chosen to be the irrotational value plus the rotational energy. These conditions are reflected by

$$\begin{aligned} \psi &= b\sin(\theta) \\ c &= \Omega\cos^2(\theta) \\ H &= H_o + \frac{1}{2}\Omega^2\cos^2(\theta) \end{aligned} \tag{4.30}$$

where $H_o = .75$ is the value of the spherically symmetric case that was used previously and b is a constant. The vorticity introduced at the base s = 1

$$\zeta = -\rho_o\Omega^2\frac{\sin(2\theta)\cos(\theta)}{2b} \tag{4.31}$$

is negative. Solutions for $\Omega = 0.05$ and 0.1 are shown in figures 4.14 and 4.15. In terms of rotational kinetic energy compared to the gravitational potential energy these are about 100 and 400 times the

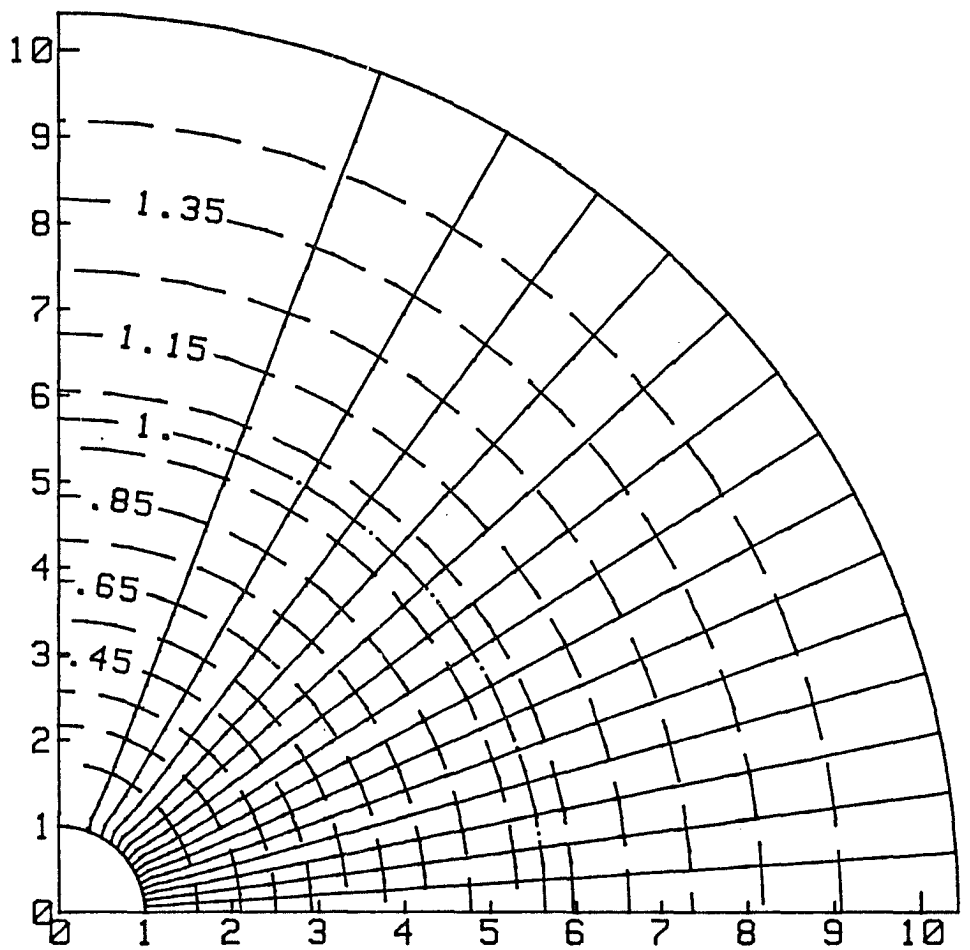


Fig. 4.14 An $\Omega = 0.05$ rotating solar wind model --- The rotation causes the flow to bend towards the pole causing a "kink" to form. Low resolution is the reason for the apparent discontinuity.

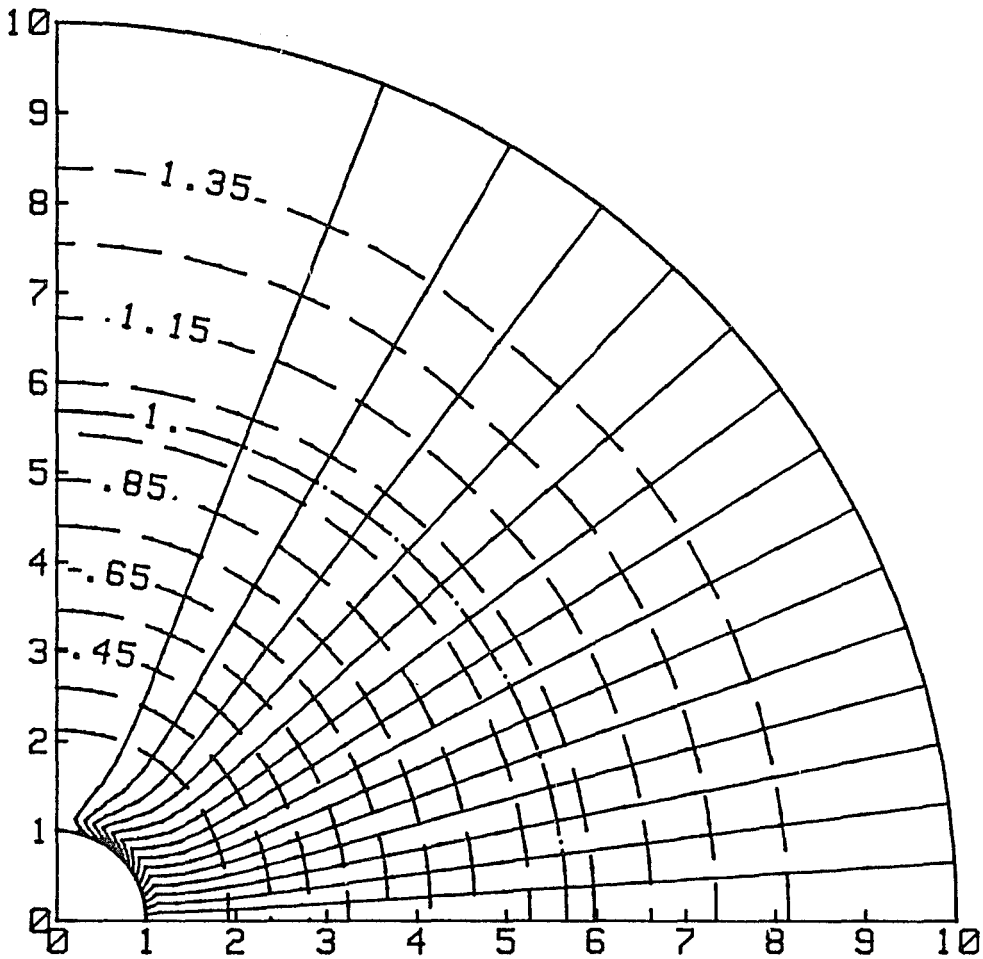


Fig. 4.15 An $\Omega = 0.1$ rotating solar wind model --- a) The full flow.

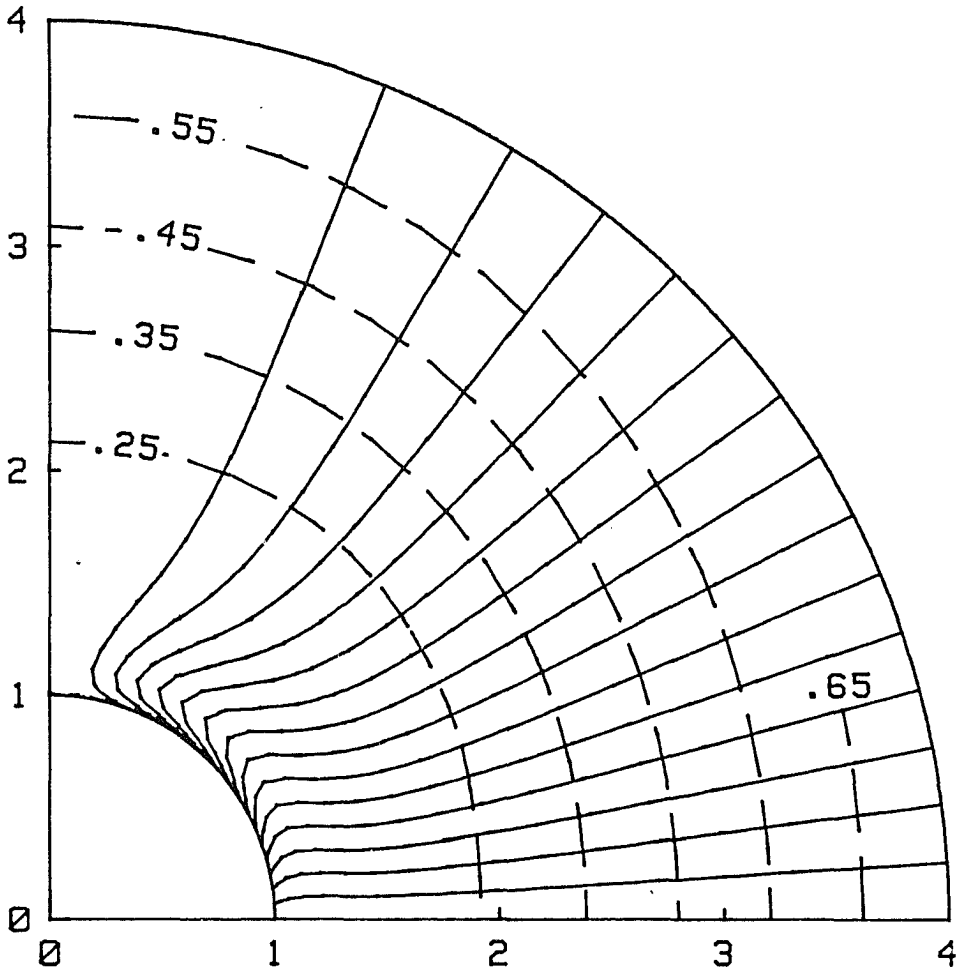


Fig. 4.15 An $\Omega = 0.1$ rotating solar wind model --- b) The "kink" better resolved.

solar values at the equator. Solutions with the solar values differ little from radial flow.

As expected, most of the variations occur near the base. Contour plots of the vorticity show that by s = 1.5 the vorticity is negligible in both cases. The decrease in the Mach number evident near the base is due to the fact that the velocity is dominated by the azimuthal component which drops as $s^{-1}$. Finally, the vorticity does change sign around s = 1.5 but the effects are small by that distance. The apparent discontinuity in the flow in figures 4.14 and 4.15a are due to poor resolution near the base. Figure 4.15b is a better resolved case of fig. 4.15a.

The "kink" of the flow in the poleward direction apparent in figs. 4.14 and 4.15 is due to the vorticity term in eqn. (4.19) and not to the centrifugal force terms. If the vorticity term is artificially turned off the solution still remains effectively radial; For $\Omega$= .1 the perturbation in eq. (4.21) due to the rotation is at most 1%. In fact, the effect is due to the Coriolis force and it is most easy to study the problem in a coordinate system which rotates with the surface. In that coordinate system the streamlines of figures 4.4 and 4.5 and the velocity components u and v are unchanged because of the axisymmetry. In the rotating coordinate frame the steady momentum equation is (Pedlosky, 1979 p. 45)

$$\underline{q}\cdot\nabla\underline{q} + 2\underline{\Omega} \times q = -\frac{\nabla \underline{P}}{\rho} + \nabla\Phi \qquad (4.32)$$

where $\underline{\Omega}$ = $(\cos(\theta),\sin(\theta),0)$ is the angular velocity vector. The

local Rossby number, which is a measure of the importance of rotation to convection is, from Pedlosky(1979 p. 24)

$$R_o = \frac{U}{2\Omega L \sin(\theta)} \tag{4.33}$$

where U is a characteristic velocity and L is a characteristic distance over which that velocity changes. For the model shown in fig. 4.5 this quantity is about .25 for $\theta \gtrsim \pi/8$. For small Rossby number the geostrophic approximation can be made which claims that the convective term can be ignored when compared to the Coriolis term. Then

$$2\underline{\Omega} \times \underline{q} = -\frac{\underline{P}}{\rho} + \nabla\Phi \tag{4.34}$$

The azimuthal component of this is

$$2\Omega(-v\sin(\theta) + u\cos(\theta)) = 0 \tag{4.35}$$

since the problem is axisymmetric. From this form, the $\theta$ component must have the same sign as the radial component, u, which is positive. The equation (4.35) can also be derived from the equations in the inertial frame. Thus, the Coriolis term causes the flow to bend up toward the pole near s = 1 where the effects of rotation are most important.

As for the irrotational solutions, the initial values of $\psi$ were set to be constant along lines of constant $\theta$. The convergence behavior for these two solutions is very similar to that of the

irrotational ones. The supersonic zones set up almost immediately because the solutions differ little over most of the mesh from the initial guess.

## 4.4 Galaxy Models

As models of highly idealized galaxies we will use uniform density oblate spheroids. Flows for spheroids with two different eccentricities will be computed. Such models are particularly easy to work with because both the coordinate transformation and gravitational potential can be expressed analytically.

The oblate spheroidal coordinates which are used are related to a cylindrical coordinate system $(z,r,\phi)$ by

$$\begin{aligned} r &= \cos(T(Y))(F(X)^2 + E^2)^{1/2} \\ z &= \sin(T(Y))F(X) \end{aligned} \tag{4.36}$$

where $T(Y) \in [0,\pi/2]$ and $F(X) \geq 1$ are stretching functions. The scale factors for such a system are

$$\begin{aligned} h_1 &= F'\left(\frac{F^2 + E^2\sin^2(T)}{F^2 + E^2}\right)^{1/2} \\ h_2 &= T'(F^2 + E^2\sin^2(T))^{1/2} \\ h_3 &= \cos(T)(F^2 + E^2)^{1/2} \end{aligned} \tag{4.37}$$

The two cases for which solutions will be shown are for E = 2 and E = 4. The grids used are pictured in figure 4.16a,b. The boundary of both spheroids corresponds to F = 1 and the particular grids shown are for F(X) = 1 + .5X and T(Y) = (.5$\pi$/16)Y.

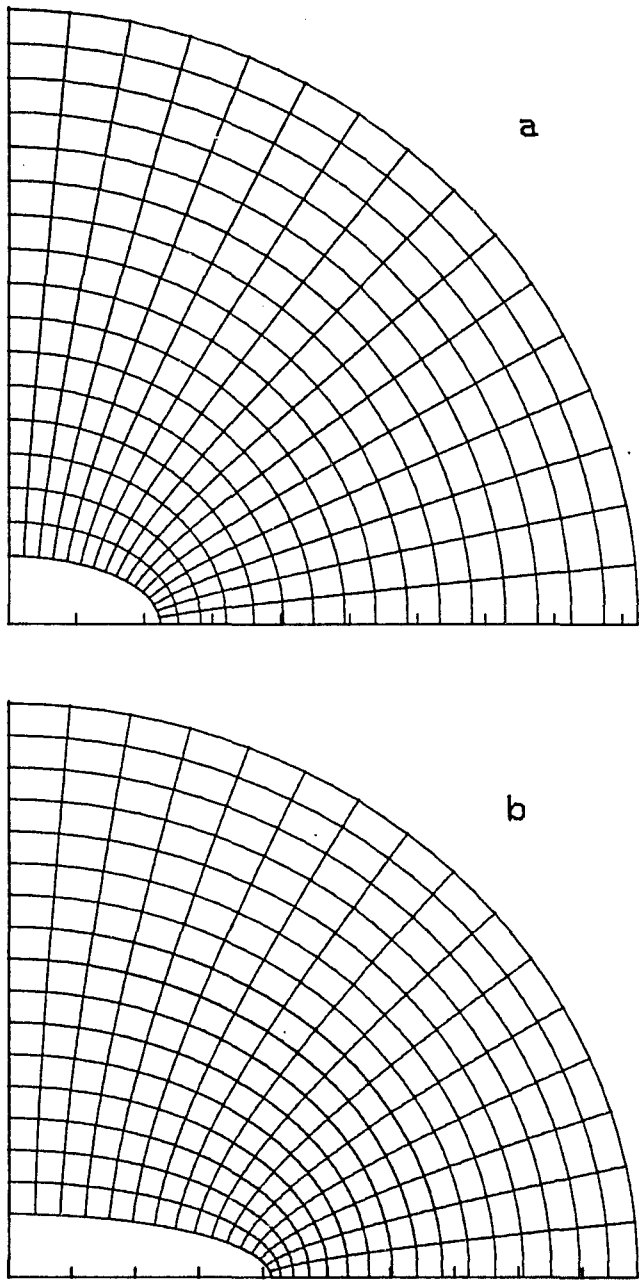


Fig. 4.16 Coordinate systems for the oblate spheroidal galaxies --- a) E = 2. b) E = 4.

The gravitational potential has been adapted to this coordinate representation from Perek(1962, p.192) and is

$$\Phi(X,Y) = -\frac{3}{4}\frac{(E^2+1)^{1/2}}{E^2}\left\{\frac{E^2-F^2}{E}\,\mathrm{Cot}^{-1}(F/E) + F - \sin^2(T)\{3F - \frac{E^2+3F^2}{E}\cot^{-1}(F/E)\}\right\} \tag{4.38}$$

The scaling is chosen so that the semi-minor axis is unity and GM= 1. Equipotential surfaces for both E = 2 and E = 4 are shown in fig. 4.17a,b. The base no longer corresponds to an equipotential surface as it does for the spherical models.

The boundary condition at the base will be that of a uniform mass flux, $\rho u$ = constant. The condition on $\psi$ is, for T' = constant,

$$\begin{aligned}\psi(T) &= bT'(1+E^2)^{1/2}\int_0^T \cos(T(y))(1 + E^2\sin^2(T(y))^{1/2}dy \\ &= \frac{b}{2}(1+E^2)^{1/2}\{\sin(T)(1+E^2\sin^2(T))^{1/2} + \\ &\quad \frac{1}{E}\log(\sin(T) + \frac{1}{E}(1+E^2\sin^2(T)) + \frac{1}{E}\log E\}\end{aligned} \tag{4.39}$$

where b is a constant which determines the total mass flux. Clearly the equations for flow from an oblate spheroid are more complex than for the solar models. Nevertheless the ideas of the last section should extend to these cases.

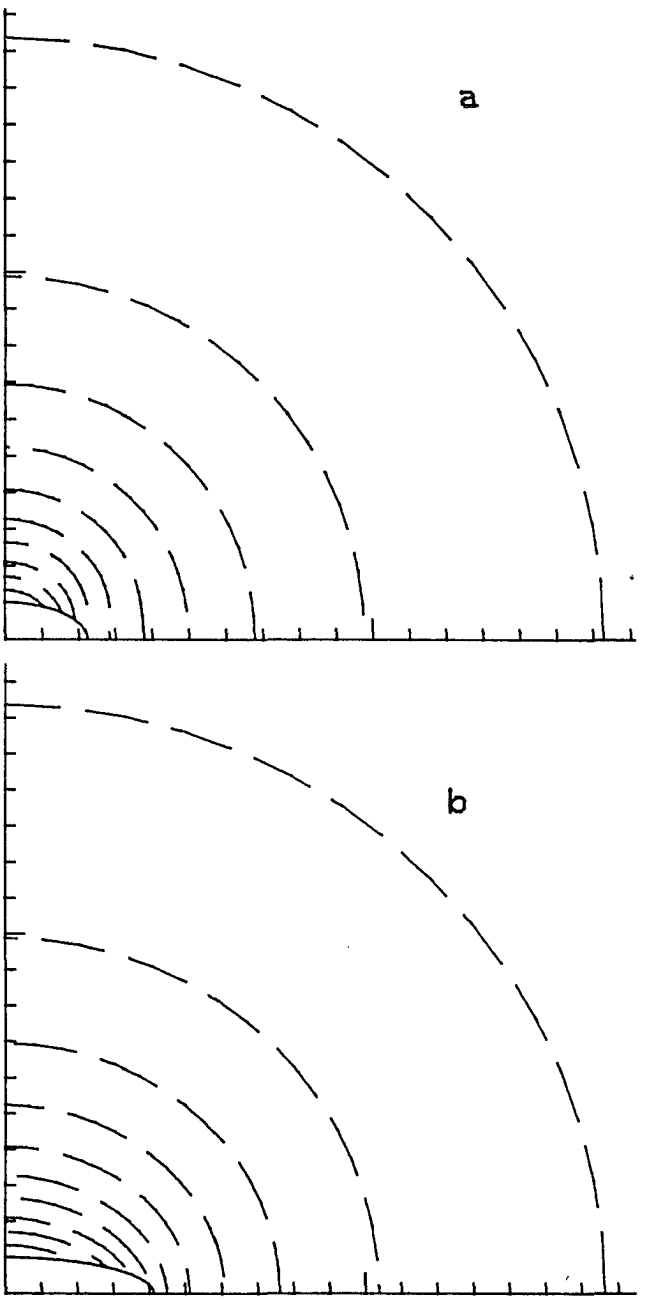


Fig. 4.17 Gravitational potentials for the oblate spheroidal galaxies ---- The equipotential curves are constant contour level differences of the potential eqn. (4.38) for a) E = 2. b) E = 4.

Irrotational Solutions

For the irrotational solutions, c = 0 and H = constant. The parameters used for the problems were chosen for convenience. For both the E = 2 and E = 4 models, $\rho_o = P_o = 1$ were used. Practical considerations influenced the choice of $\gamma = 1.4$. Because the initial values of $\psi$ are not necessarily good approximations to the exact values, the mass fluxes at a given point computed from the derivatives of $\psi$ could be out of the ranges for which values of the density exist. (See fig. 2.2.) A larger value of $\gamma$ insures a larger range of flux for which the density is defined.

The choice of H = .1 for the E = 2 and H = .17 for the E = 4 models was also motivated by practical factors. The outer boundary must be placed far enough away so that one can reasonably expect the flow to be radial. These choices approximately place the sonic line near the middle of the grids shown in fig. 4.17a,b yet - without needing a highly stretched mesh - the outer boundary is far enough from the base. As with the spherical solutions, increasing H moves the sonic line in and lowering H moves it out. This fact was used in choosing these values of H.

Figures 4.18 and 4.19 show the solutions to the two irrotational galactic wind problems. The flows are basically the same so they will be discussed together. In both cases the streamlines are bent toward the equator. The effect is more pronounced on the E = 4 solution. At the base the largest Mach number (and lowest density) occurs at the equator and decreases toward the pole. On fig. 4.18, M

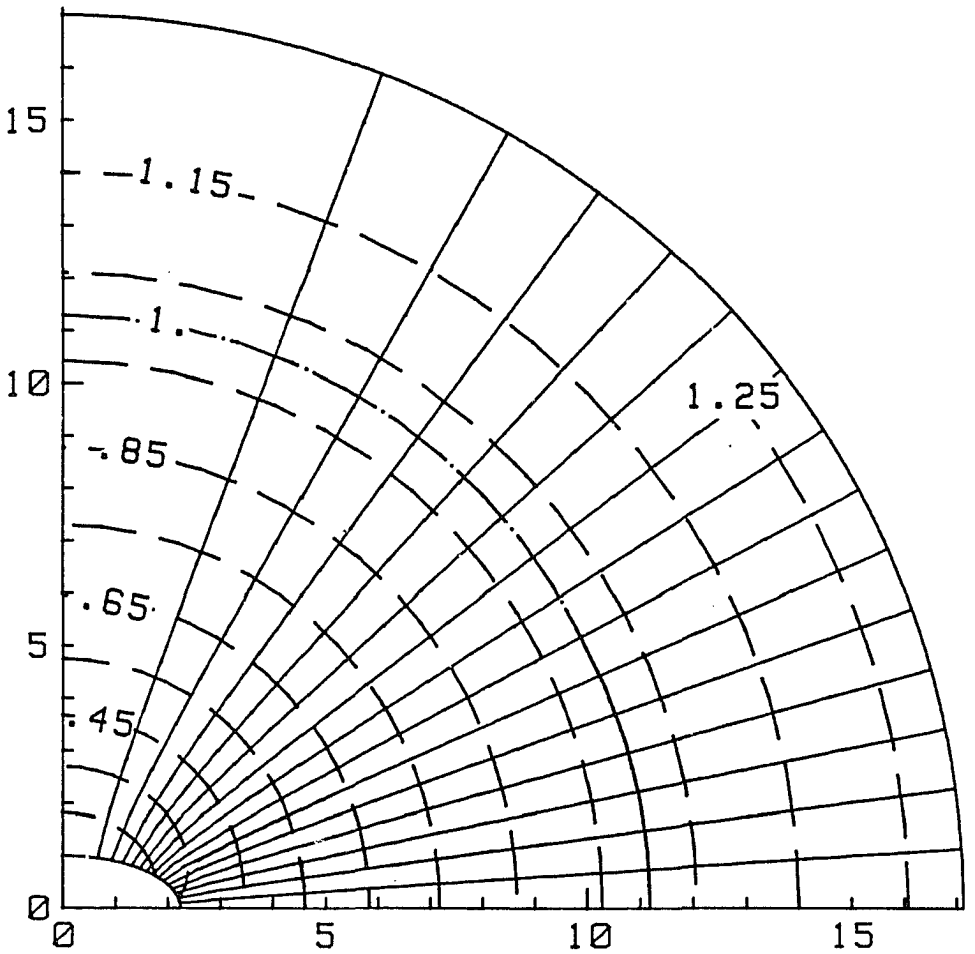


Fig. 4.18 An irrotational wind for the E = 2 model --- The flow, which has a uniform normal mass flux at the base, is bent toward the equator and the sonic line is nearly circular.

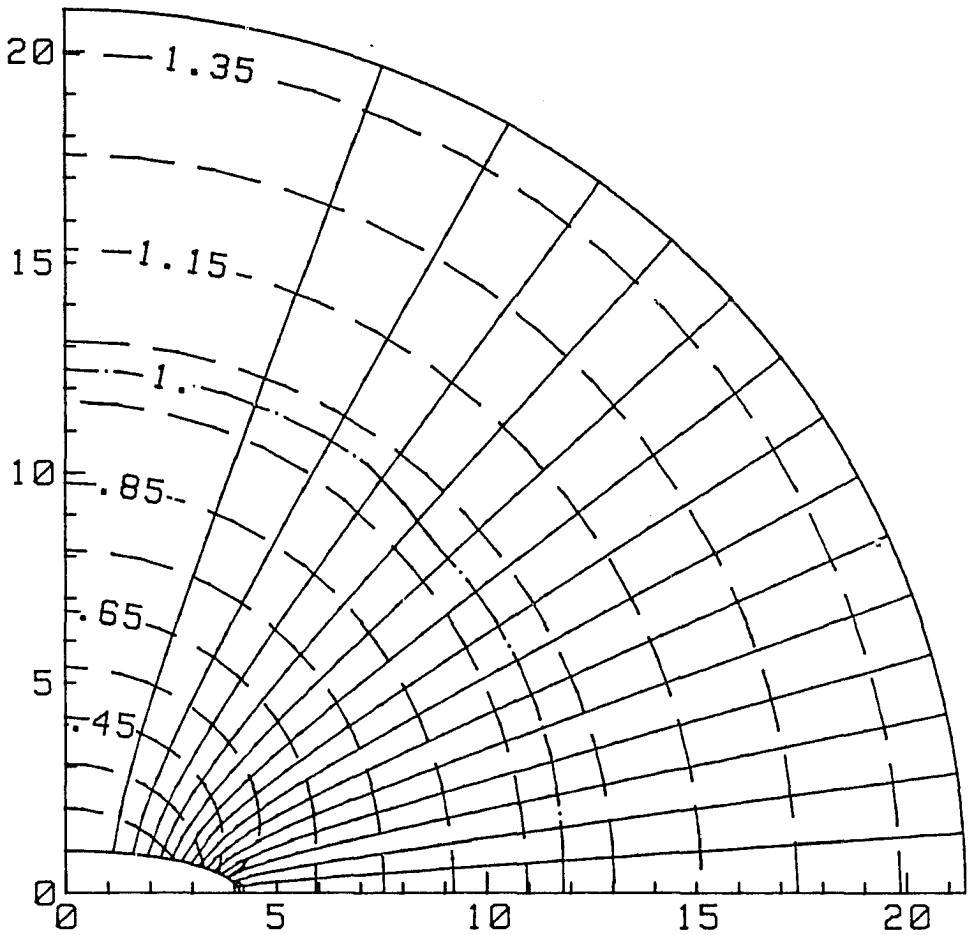


Fig. 4.19 An irrotational wind for the E = 4 model --- As with the solution of fig. 4.18, the sonic line is nearly circular. The normal mass flux at the base is constant.

ranges from 0.35 to 0.15 while for E = 4 the range is 0.7 to 0.16. The difference in these is due to the fact that the gravitational potential varies by a larger amount along the base for the E = 4 problem. Nevertheless, the flows are accelerated so that the sonic line in both cases is nearly circular.

An important difference between these models and the spherical model used in the last two sections is that the density does not vary as rapidly near the base. For instance, $d\rho/dz < .1$ for the E = 4 solution along the polar axis. This is a far different behavior than that seen in fig. 4.4. Thus we expect that for the rotational flows the effects of vorticity will be spread over a larger area than in the solar models. Furthermore, the density values at the base for the galaxy models are much lower than the base density in the spherical models. For the E = 2 model the density at the base varies from 0.07 at the equator to 0.14 at the pole and for E = 4 the variation is from 0.07 to .23. Then since $\zeta \propto \rho$ we would also expect the effects of the vorticity introduced, say, by the rotating body to be not as violent as are seen in the solar models.

The initial values of $\psi$ for these computations were that $\psi$ = constant along lines of constant Y. The convergence behavior was very similar to that of the two-dimensional irrotational solutions for the solar wind models shown in fig. 4.13.

Rotational Flows

For the rotational flows we use

$$H = H_o + 1/2\ w^2$$

$$c = \Omega h_3^2$$

where $H_o$ is the value used for the irrotational solutions. The values of $\Omega$ used were 0.05 for E = 4 and 0.1 for E = 2. This sets up the flow with approximately the same amount of rotational kinetic energy at the equator for both problems.

Before discussing the solutions themselves, we note that rotational flows are much harder to compute than the irrotational ones. First, since H and c depend on $\psi$, the initial guess for $\psi$ must be good. Most often the same values used for the irrotational problems would produce density values so unrealistic that the residuals would "blow up" within one to four iterations. We have had the best success by using the converged irrotational solution as the starting values of the rotational flows. Next, the convergence rates and solutions are much more sensitive to the mass flux in rotational problems than they are for irrotational ones. One reason is that H, which is now a function of $\psi$, determines the position of the sonic line. The reason no difficulties showed up in the rotational flows of the last section was because the variation of H with $\theta$ was only 0.7% over the base while for these problems it is 25% for the E = 2 and 12 1/2% for the E = 4. Not surprisingly, the E = 2 solution was the hardest to obtain. Finally, because of the sensitivity to the mass

flux the sonic lines for the rotational flows are not as smooth as for the irrotational ones.

The solutions for the rotating galaxy models are shown in figures 4.20 and 4.21. The streamlines look very similar to those of the irrotational flows. Close examination shows that, like in the rotating spherical winds, the streamlines are bent toward the pole. The reason for the less drastic behavior has already been discussed. The effects on the Mach number curves are more obvious, though. The perturbation of H is largest at the equator and goes to zero at the pole. As one might expect form previous discussions, the sonic line is moved in toward the body mostly near the equator causing it to look like a prolate ellipse rather than a circle. The effect is mostly due to the variation of H rather than to the contribution to M of the azimuthal velocity component, w, because at that radial distance w is small.

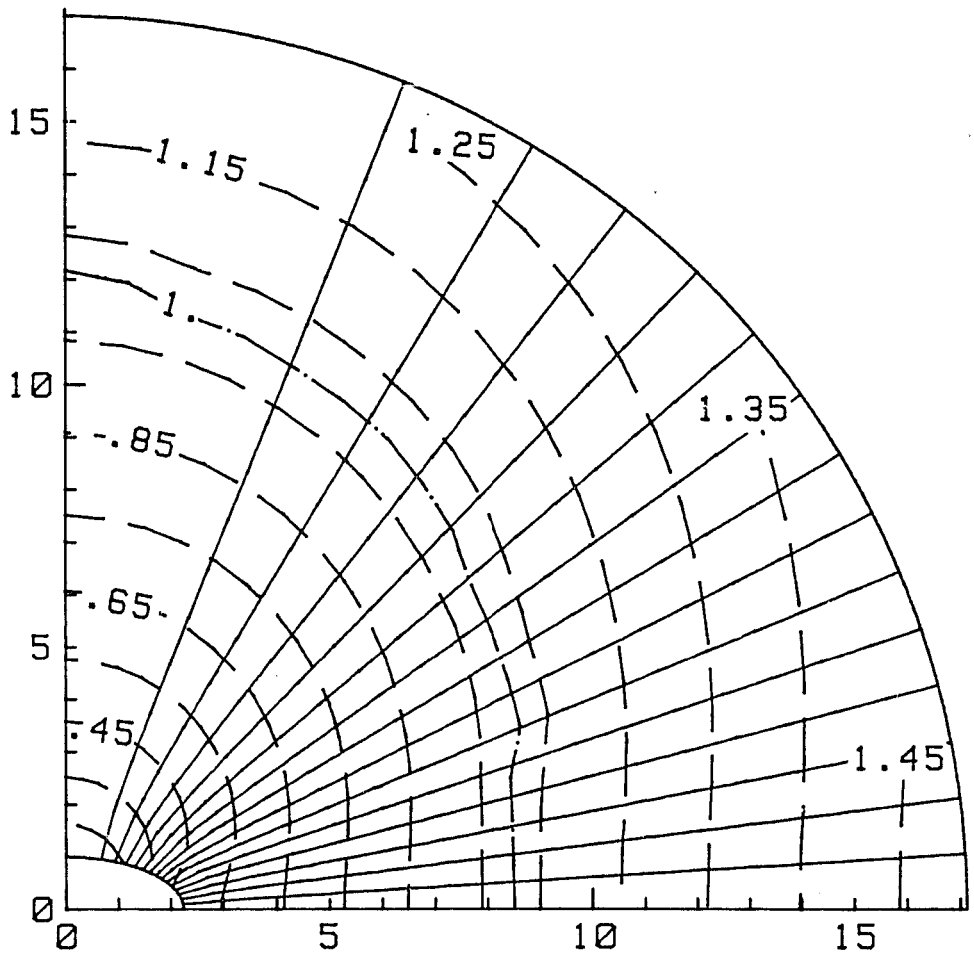


Fig 4.20 A rotational wind with $H = H_o + 1/2w^2$ for the E=2 model --- The angular frequency is $\Omega = 0.05$. The effect of the variation in H is that the sonic line moves in more toward the equator.

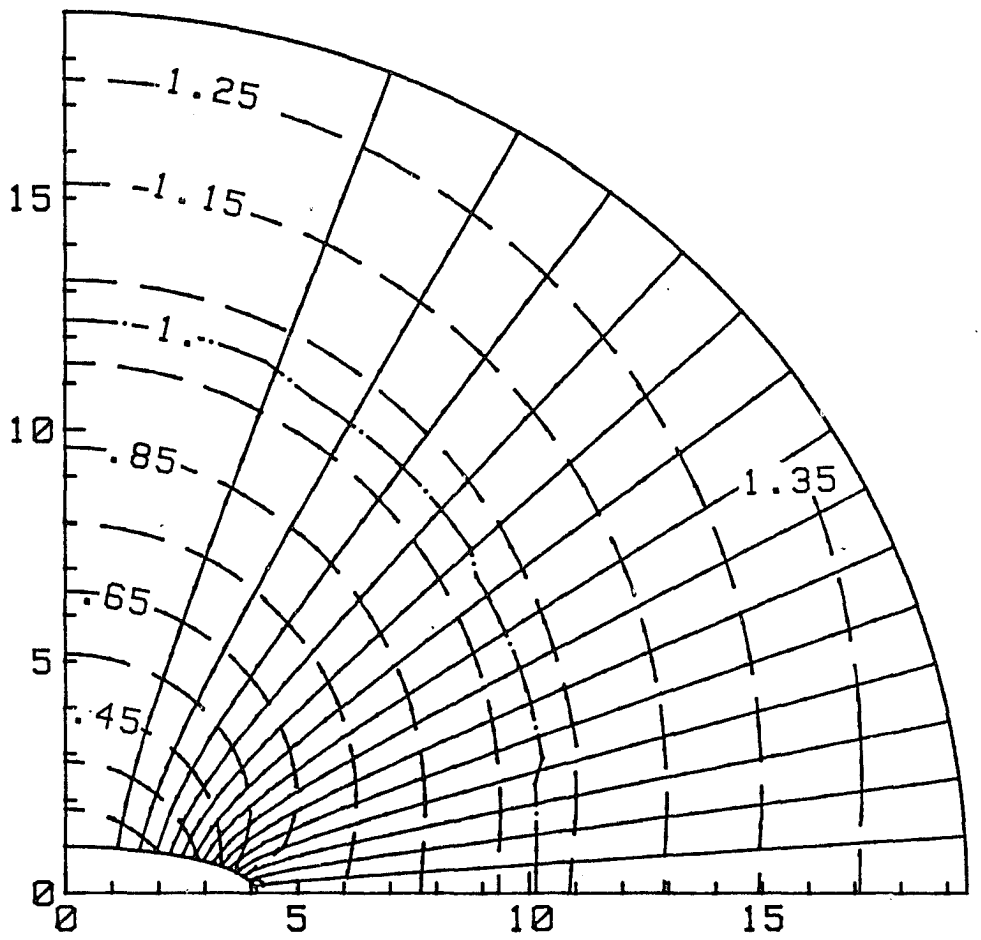


Fig 4.21 A rotational wind with $H = H_o + 1/2w^2$ for the E = 4 model --- The angular frequency $\Omega = 0.1$. The sonic line is again moved inwards predominantly near the equator to create a prolate sonic line.

# CHAPTER 5

## SUMMARY AND CONCLUSIONS

The introduction of a stream function to reduce the continuity and momentum equations to a single second order partial differential equation is a completely general procedure for two-dimensional axisymmetric problems. We have shown how to apply this technique to a class of problems motivated by the theory of the steady solar wind. The stream function equation itself can be solved by applying ideas developed for the transonic potential equation and we have presented a method for computing the density through Bernoulli's equation.

In the Introduction we mentioned the advantages of reducing the steady flow problem to a single PDE coupled with an algebraic equation for the density. First, the numerical procedure is fast. For example, 30 iterations on a 32x18 mesh for the rotational E = 4 galactic wind takes 10 seconds on a CDC Cyber 175. The method is slower than a similar potential formulation would be only because the density must be solved for iteratively.

For the wind problems, the stream function formulation allows the extension of the ideas from one dimensional theory. Also, qualitative analysis of the equations is far simpler than when using the primitive variables. The effects of rotation and the variation of the total enthalpy of the inflowing gas, for instance, are explicit in

the equations. Perturbation techniques should be easier to apply on this equation, too.

Accurate solutions of solar wind-type problems can be computed with few grid points because the density is determined from an algebraic equation rather than a differential equation. Also, though the velocities may vary greatly over the mesh, the stream function is bounded by the values on the boundaries and hence can be more accurately approximated.

There are, however, some operational difficulties with the technique we have used here. The greatest difficulty is that of finding the proper mass flux to obtain the transonic solution for a particular problem. Our procedure of computing a solution, examining it, and changing the mass flux requires too much user interaction. What would be desirable is an automatic way of computing the needed mass flux as part of the solution process. Also, the algorithm is not robust in the sense that for some initial values of the stream function the relaxation procedure blows up because reasonable density values cannot be found. The problem shows up particularly when rotational flows are solved.

Another difficulty with the technique as described here is that the initial conditions must be chosen carefully. There do not exist values of the density for all values of the stream function and its derivatives. This is especially true for rotational flows where c and H are both functions of $\psi$. One approach which we have used to

avoid this problem is to use the solution to another problem such as an incompressible flow as the initial guess for a compressible one.

Finally, though the boundary conditions are useful for theoretical studies they are not necessarily the most convenient. In this formulation either the stream function or its normal derivative corresponding to the normal or tangential mass flux must be specified along the inflow boundary. In addition, H and c are specified there. The pressure and density are then computed as part of the solution. In many ways it is more natural to specify P and $\rho$ and let the mass flux be adjusted as part of the solution. This would require a time dependent approach.

Because this is the first time the steady two-dimensional wind type flows have been looked at directly with a stream function technique, we have only explored some simple model problems. In addition to the radial flow problem for the solar wind we have also presented irrotational solutions which show the effect of regions having higher and lower mass flux. To further test the code the test cases were ones where the behavior in latitude could be determined. The most interesting solutions were those of the rapidly rotating solar type problems. Contrary to intuition the flow is bent toward the pole because the coriolis force is more important than the centrifugal force.

For galactic wind problems we examined the flow from two oblate spheroidal bodies. Both rotational and irrotational flows were computed. It is interesting to note that even for the non-rotating problems the flow is bent towards the equator. The effect is greater

for the more flattened spheroid. Also, the sonic surface is basically spherical even though the flow is not.

In the context of these simple models there is much left to do. For example, with the presence of vorticity the possibility of separated flows arises. We have computed examples where H only was varied that had a recirculation region near the base of a spherical model. From the discussion of section 2.3 it is difficult to define the vorticity in a circulation region where streamlines do not cross the boundaries. It would be interesting to see under what situations - realistic or not - that such flows can develop. Also, for galaxy models we have not presented solutions of very flattened oblate spheroids. From figures 4.18 and 4.19 we commented that the inflow mach number at the equator is larger for the more flattened of the two. It appears that this is a trend and that for very flat cases the flow would have to be supersonic near the equator as it exits the base. We only mention the observation because exactly what is causing the behavior is not yet known.

Because the models used were so simple it is impossible to say if the solutions presented correspond to any real flows. The kink effect for the rotating solar models, for instance is the result of an extremely fast rotation. Even so, the presence of magnetic fields would probably change the results substantially. For the galaxy models one would have to decide whether a uniform density oblate spheroid with a uniform outward mass flux adequately represents the flow from a galaxy. Certainly more realistic sources and gas-dynamics

must be used before too much can be said about the relevance of our solutions.

The study of winds, then, is certainly not complete. We have presented an approach and a technique which might be used by others to study in more detail the types of problems covered by the simple theory. We hope some of our results will motivate further and more detailed studies of these problems.

REFERENCES


Ballhaus, William F., Jameson, Anthony, and Albert, J.(1978) "Implicit Approximate Factorization Schemes for the Efficient Solution of Steady Transonic Flow Problems" AIAA J. 16 pp. 573-579

Bardeen, James M. and Berger, Beverly K.(1978) "A Model for Winds from Galactic Disks" Ap.J. 221 pp. 105-113

Batchelor, G.K.(1967) Introduction to Fluid Dynamics Cambridge Univ. Press.

Black, Davis C and Bodenheimer, Peter(1975) "Evolution of Rotating Interstellar Clouds. I. Numerical Techniques" Ap.J. 199 pp. 619-632

Bregman, Joel N.(1978) "Galactic Winds and the Hubble Sequence" Ap.J. 224 pp. 768-781

Burke, J. Anthony(1968) "Mass Flow from Stellar Systems - I Radial Flow from Spherical Systems" Mon. Not. Roy. Ast. Soc. 140 pp. 241-254

Chamberlain, J.W.(1961) "Interplanetary Gas.III. A Hydrodynamic Model of the Corona" Ap.J. 133 pp. 675-687

Chin, W.C. and Rizetta, D.P.(1979) "Airfoil Design in Subcritical and Supercritical Flows" J. Appl. Mech. 46 pp. 761-766

Courant, Richard and Hilbert, David(1962) Methods of Mathematical Physics Vol. II. New York:Interscience

Courant, Richard and Friedrichs, K.O.(1948) Supersonic Flow and Shock Waves New York:Springer-Verlag

Emmons, Howard W.(1944) "The Numerical Solution of Compressible Fluid Flow Problems" NACA TN 932

Emmons, Howard W.(1946) "The Theoretical Flow of a Frictionless, Adiabatic gas Inside of a Two-Dimensional Hyperbolic Nozzle" NACA TN 1003

Emmons, Howard W.(1948) "The Flow of a Compressible Fluid past a Symmetrical Airfoil in a Wind Tunnel and in Free Air" NACA TN 1746

Endler, F.(1971) "Interaction Between the Solar Wind and Coronal Magnetic Fields" Ph.D. Thesis, Gottingen University

Habe, Asao and Ikeuchi, Satoru(1980) "Dynamical Behavior of Gaseous Halo in a Disk Galaxy" Prog. Theor. Phys. 64 pp. 1995-2008

Hafez, Mohammed(1979) "Numerical Solution of Transonic Full Stream Function Equations in Conservation Form" Flow Res. note #178

Hafez, Mohammed and Lovell, Donald(1981) "Numerical Solution of Transonic Stream Function Equation" AIAA 5th Computational Fluid Dynamics Conference, June 22-23 Palo Alto, Ca. AIAA Paper 81-1017 pp. 364-372

Hall, M.G.(1981) "Computational Fluid Dynamics - A Revolutionary Force in Aerodynamics" AIAA 5th Computational Fluid Dynamics Conference, June 22-23, 1981. AIAA Paper 81-1014 pp. 176-188

Holzer, Thomas E. and Axford, W.I.(1970) "The Theory of Stellar Winds and Related Flows" Ann. Rev. Astr. and Ap. 8 pp. 31-60

Hundhausen, A.J.(1972) Coronal Expansion and Solar Wind New York:Springer-Verlag

Ipavich, Fred M.(1975) "Galactic Winds Driven By Cosmic Rays" Ap. J. 196 pp. 107-120

Jameson, Anthony(1974) "Iterative Solution of Transonic Flows Over Airfoils and Wings, Including Flows at Mach 1" Comm. Pure and Appl. Math 27 pp. 283-309

Johnson, H.E. and Axford, W.I.(1971) "Galactic Winds" Ap. J. 165 pp. 381-390

Lax, Peter D.(1973) Hyperbolic Systems of Conservation Laws and the Mathematical Theory of Schock Waves Philadelphia:SIAM

Lin, C.C. and Rubinov, S.I.(1948) "On the Flow Behind Curved Shocks" J. of Math. and Physics 27 pp. 105-129

Lomax, Harvard(1981) "Some Prospects for the Future of Computational Fluid Dynamics" AIAA 5th Computational Fluid Dynamics Conference, June 22-23, Palo Alto, Ca. AIAA Paper 81-0994 pp. 3-15

Matthews, William G. and Baker, James C.(1971) "Galactic Winds" Ap. J. 170 pp. 241-259

Murman, E.M. and Cole, J.D.(1971) "Calculation of Plane Steady Transonic Flows" AIAA J 9 pp. 114-212

Oliger, Joseph and Sunstrom, Arne(1978) "Theoretical and Practical Aspects of some Initial Boundary Value Problems in Fluid Dynamics" SIAM J. Appl. Math 35 pp. 419-446

Parker, Eugene(1958) "Dynamics of the Interplanetary Gas and Magnetic Fields" Ap. J. 128 pp. 664-675

Parker, Eugene(1963) Interplanetary Dynamical Processes New York:Interscience

Parks, P.B. and Turnbull, R.J.(1978) "Effect of Transonic Flow in the Ablation Cloud on the Lifetime of a Solid Hydrogen Pellet in a Plasma" Phys. Fluids 21 pp. 1735-1741

Pedlosky, Joseph(1979) Geophysical Fluid Dynamics New York:Springer-Verlag

Perek, L.(1962) "Distribution of Mass in Oblate Stellar Systems" in Advances in Astronomy and Astrophysics Vol. 1 New York:Academic Press, pp. 165-287

Pizzo, Victor(1978) "A Three-Dimensional Model of Corotating Streams in the Solar Wind.1.Theoretical Foundations" J. Geophys. Res. 83 p. 5563-5572

Pizzo, Victor(1980) "A Three-Dimensional Model of Corotating Streams in the Solar Wind.2. Hydrodynamic Streams" J. Geophys. Res 85 pp. 727-743

Pizzo, Victor(1981) "A Three-Dimensional Model of Corotating Streams in the Solar Wind.III. Magnetohydrodynamic Streams" Preprint

Pneuman, G.W. and Kopp, R.A.(1971) "Gas-Magnetic Field Interactions in the Solar Corona" Solar Physics 18 pp. 258-270

Sanders, R.H. and Prendergast, K.H.(1974) "The Possible Relation of the 3-Kiloparsec Arm To explosions in the Galactic Nucleus" Ap.J. 188 pp. 489-500

Siscoe, G.L. and Finley, L.(1969) "Meridional (north-south) Motions of the Solar Wind" Solar Physics 9 pp. 452-466

Schmilovich, Arvin and Caughey, David(1981) "Application of the Multi-grid method to Calculation of Transonic Potential Flow about Wing-Fuselage Combinations" NASA CP 2202 pp. 101-130

Van Albada, G.D., Van Leer, B. and Roberts Jr., W.W.(1981) "A Comparative Study of Computational Methods in Cosmic Gas Dynamics" ICASE rept. 81-24

Yu, N.J., Seebass, A.R. and Ballhaus, W.F.(1978) "Implicit Shock Fitting Scheme for Unsteady Transonic Flow Computations" AIAA J. 16 pp. 673-678